The progress of the model development on ELM control with RMP and RF waves in ASIPP

Presenter: T.Y. Xia[1*]

Y.L. Li[1], B. Gui[1], J.X. Li[1,2], H.M. Qi[1,2], Y.D. Yu[1,2], Y.Q. Huang[3] , Y.B. Wu[4], and EAST Team[1]

[1]ASIPP, [2]USTC, [3]Hengyang Normal University, [4]Anqing Normal University

*E-mail: xiaty@ipp.ac.cn

*This work was supported by National Key R&D Program of China under Grant No. 2017YFE0301100, 2017YFE0301101, and 2014GB106001. The China Natural Science Foundation under Contract No.11675217 and 11505236. This work is also sponsored in part by Youth Innovation Promotion Association Chinese Academy of Sciences (2017479) and K.C. Wong Education Foundation. Numerical computations were performed on the ShenMa High Performance Computing Cluster in Institute of Plasma Physics, Chinese Academy of Sciences.

Outline

- Motivation
- Modeling for RF effects on ELM control
- Modeling for magnetic topology on ELM control
- summary

ASIPP

EAST aims at high performance & long pulse operation, The RF waves are necessary for the current driving & heating

Long Pulse: hundreds of seconds

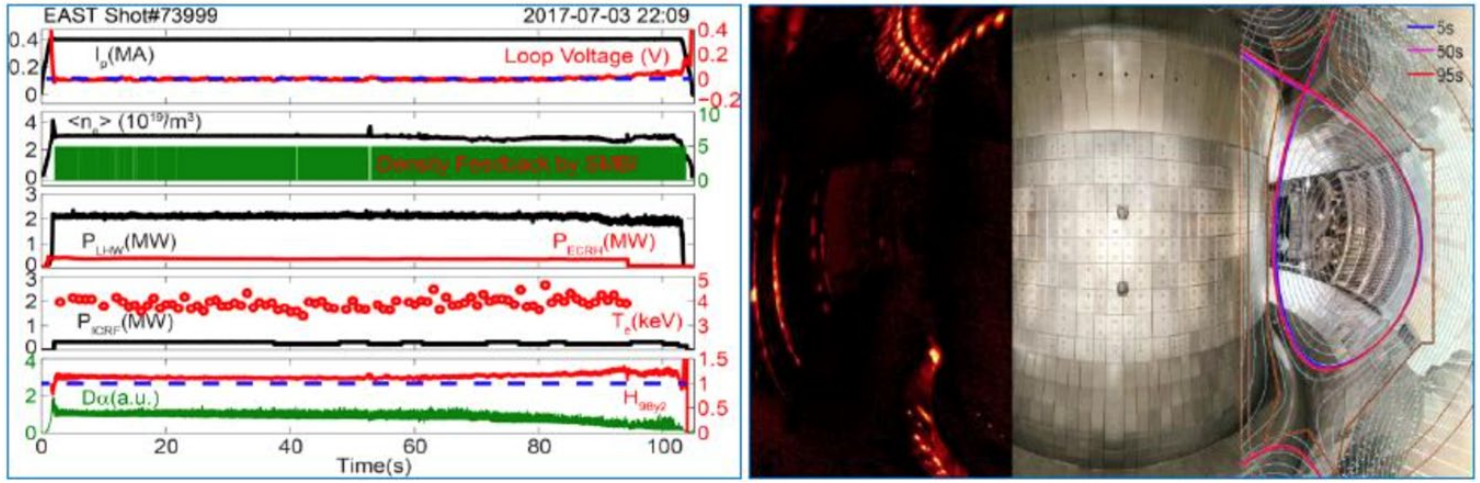

High β_p

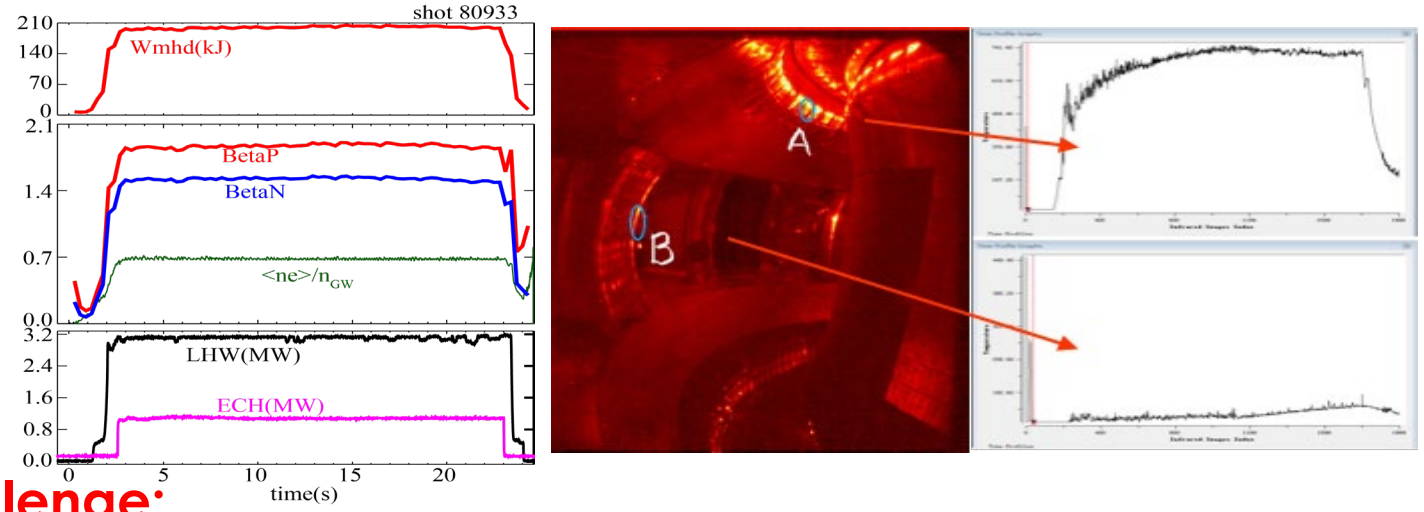

- **Challenge:**
  - **Avoidance of large ELMs**
  - **Low peak heat load/Tolerable transient heat shock**

ASIPP

Motivation: Understanding the physics of ELM control on EAST

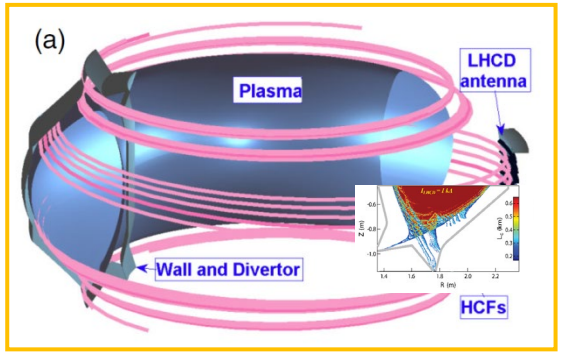

Lower Hybrid wave (LHW) [Liang Y. *et al*, PRL (2013)]

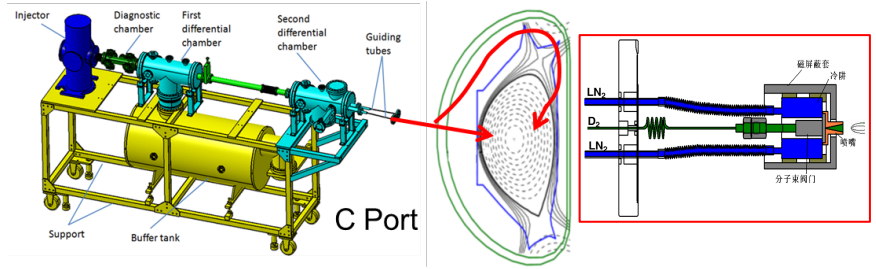

Pellet, super-sonic molecular beam injection (SMBI)

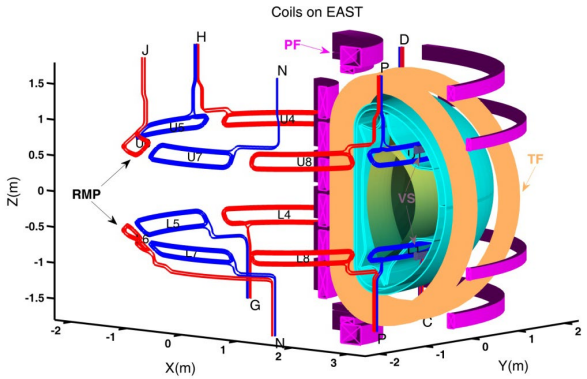

Resonant magnetic perturbation[Sun Y. *et al*, PRL (2016)]

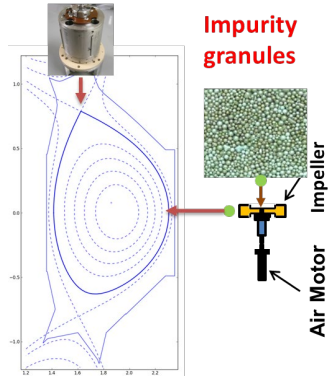

Lithium injection [Hu J. *et al*, PRL (2015)]

- EAST is the tokamak which can be operated under the ITER-like long-pulse, low rotation and metal wall conditions with RF dominant heatings.
- Various ways of ELM control have been developed on EAST successfully.

ASIPP

Outline

- Motivation
- **Modeling for RF effects on ELM control**
- Modeling for magnetic topology on ELM control
- summary

ASIPP

The effects of RF waves on edge instabilities

➢Indirect effects: Kinetic equilibrium

- ☐ Heating: profiles
- ☐ Current driving: magnetic shear
- ☐ Ponderomotive force: rotation
- ☐ …

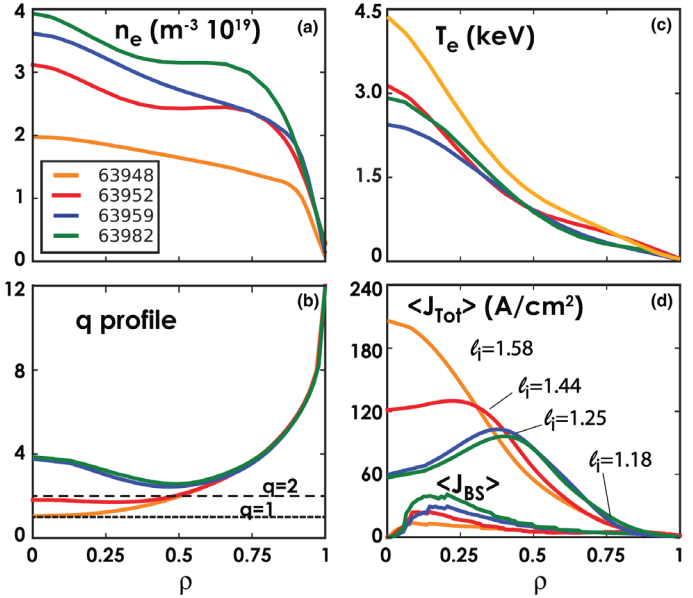

A. Garrofallo et al., NF 57 076037 (2017)

➢Direct effects:

- ☐ Current driving: topology
- ☐ RF sheath: SOL rotation
- ☐ Source terms
- ☐ …

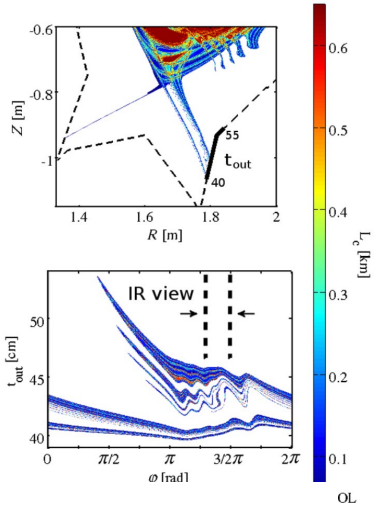

Y.F. Liang et al., PRL 110, 235002 (2013).

$$m_s n_s\left(\frac{\partial \mathbf{V}_s}{\partial t}+\mathbf{V}_s\cdot\nabla\mathbf{V}_s\right)=n_s q_s(\mathbf{E}+\mathbf{V}_s\times\mathbf{B})-\nabla p_s$$
$$-\nabla\cdot\pi_s+\mathbf{R}_s+\mathbf{F}^{\mathrm{rf}}_{s0},$$

$$\frac{3}{2}n_s\left(\frac{\partial T_s}{\partial t}+\mathbf{V}_s\cdot\nabla n_s\right)+n_s T_s\nabla\cdot\mathbf{V}_s$$
$$=-\nabla\cdot\mathbf{q}_s-\pi_s:\nabla\mathbf{V}_s+Q_s+S^{\mathrm{rf}}_{s0}.$$

C.C. Hegna & J.D. Callen, PoP 16, 112501 2009

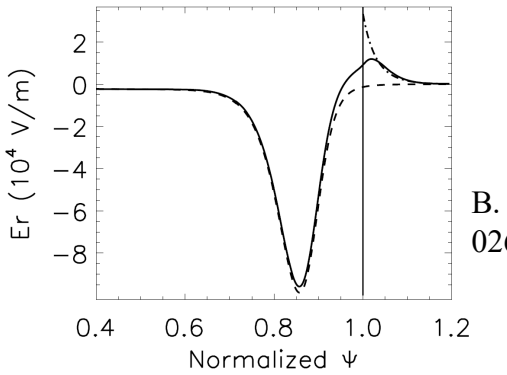

B. Gui et al., NF 58 026027 (2018)

ASIPP

Outline

- Motivation
- **Modeling for RF effects on ELM control**
  - ✓ **Indirect effects by RF**
  - ✓ Direct effects by RF
- Modeling for magnetic topology on ELM control
- summary

ASIPP

The frequency and poloidal wavenumber of the coherent mode at EAST pedestal are reproduced by the simulations

Validations on coherent mode:

- Similar calculation of f and k
- Simulated frequency is close to exp.
- k_θ is in the range of exp. (0.5-0.7cm^{-1})
- Density fluctuations rotate in the electron diamagnetic direction
- The simulated fluctuations are in the similar amplitude with exp.

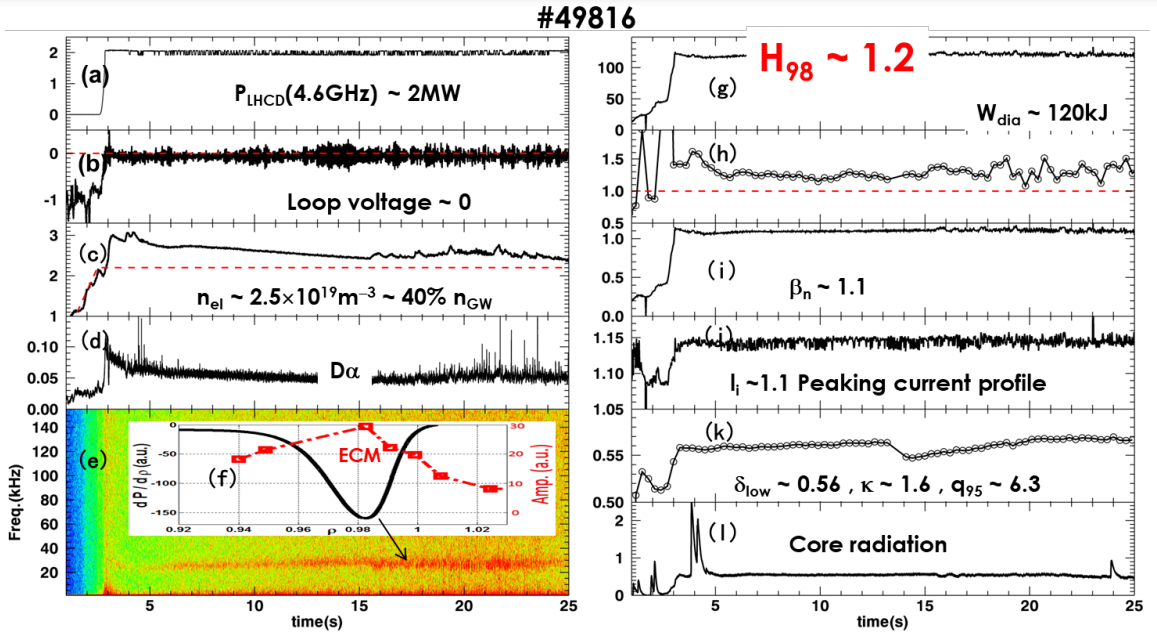

H. Q. Wang, et al., PRL, 112 185004 (2014)

EAST diagnostic

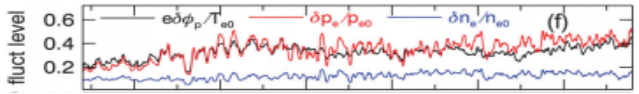

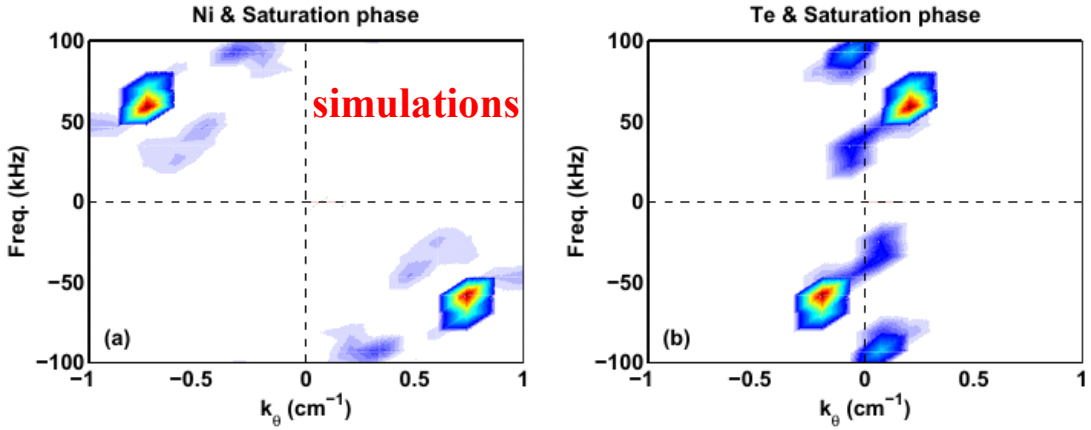

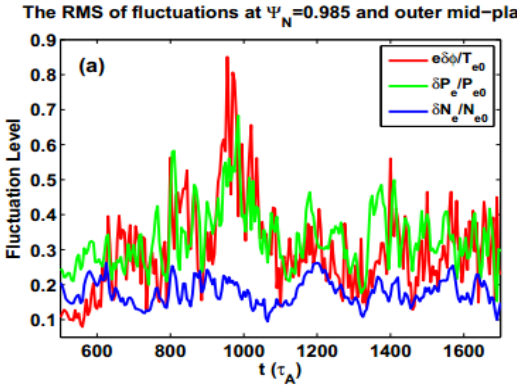

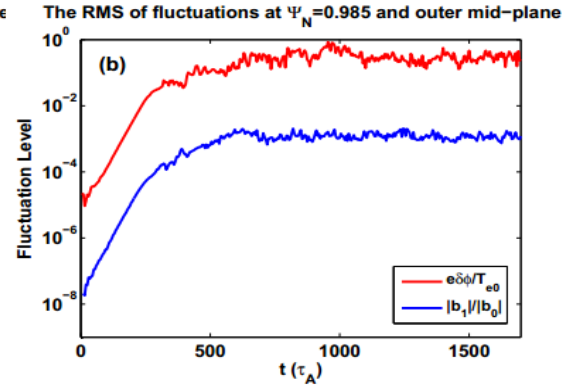

ASIPP

The simulated poloidal mode structures qualitatively agree with ECEI diagnostic

simulations

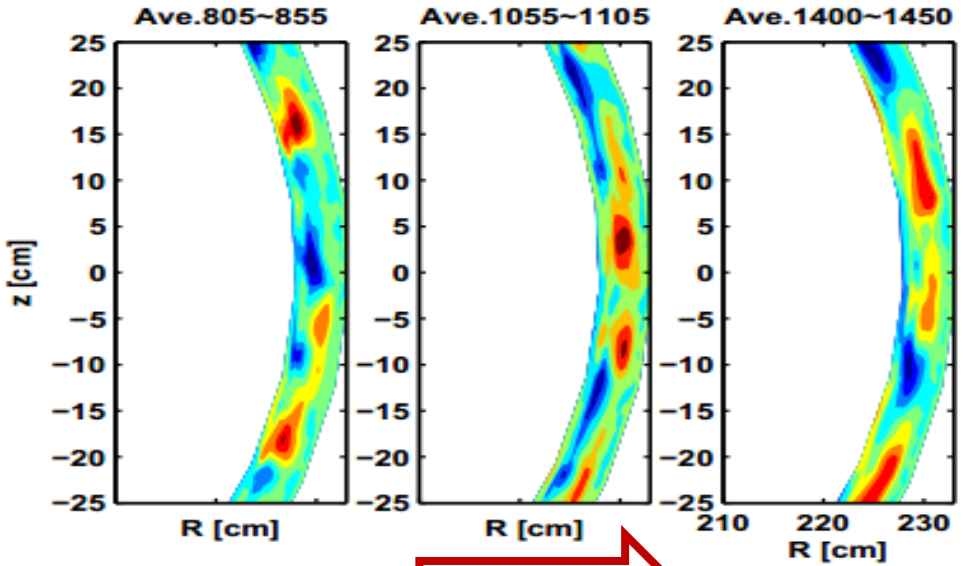

ECEI

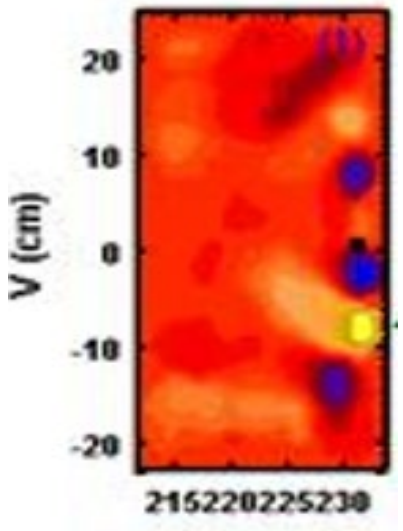

- The simulated toroidal mode structure shows the similar numbers
- The radial extension is narrower due to the noise of diagnostic (M. Kim, NF 2014)
- The poloidal extension is longer, smaller Te wavenumber in simulation.

ASIPP

Outline

- Motivation
- **Modeling for RF effects on ELM control**
  - ✓ Indirect effects by RF
  - ✓ **Direct effects by RF**
    - **HCF, CM & sheath effects**
- Modeling for magnetic topology on ELM control
- summary

ASIPP

Lower-hybrid waves show suppression effects on ELMs in EAST & HL-2A

LHWs suppress & mitigate ELMs

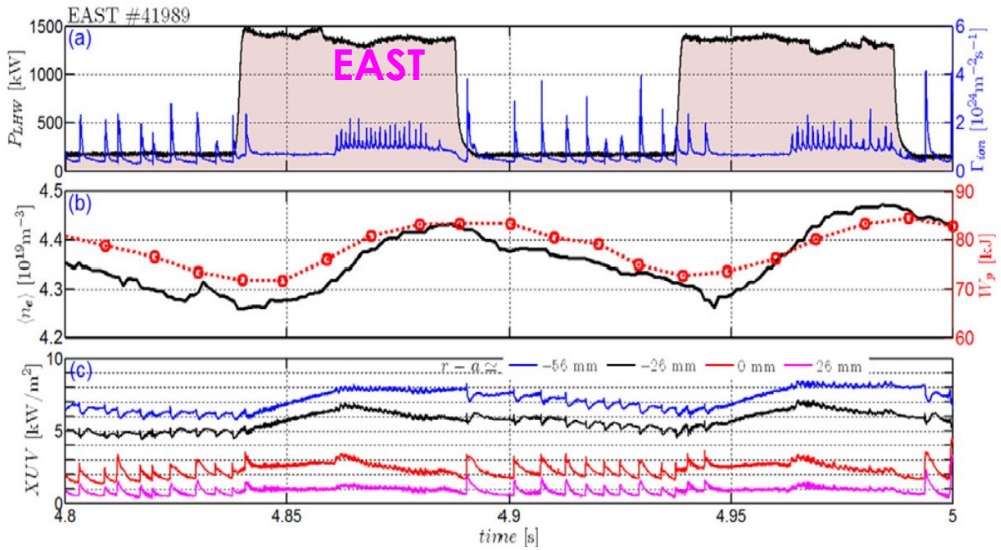

R. Chen, et al., Nucl. Fusion 55 (2015) 033012

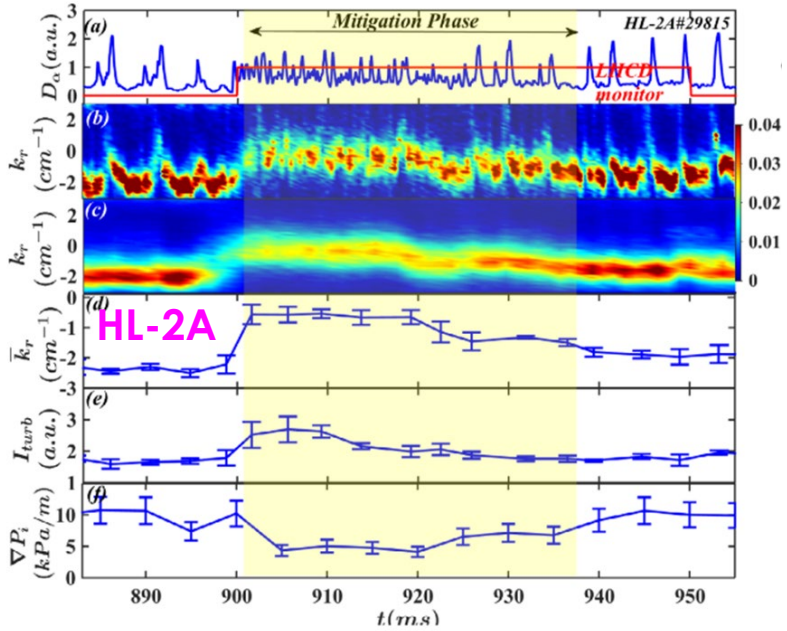

G.L. Xiao, et al., Nucl. Fusion 59 (2019) 126033

ASIPP

LHW drives the helical current filaments (HCF) in SOL and changes the edge magnetic topology

1. HCFs by LHW are able to change the edge magnetic topology and broaden the expansion on divertor.

2. The total HCF current ~1.3kA.

3. HCFs dominated by n=1 due to the geometric effect of the LHW antenna, but n>1 used in the simulation due to the efficiency

4. A modeled HCF in SOL is added into BOUT++ as the extra magnetic flutter.

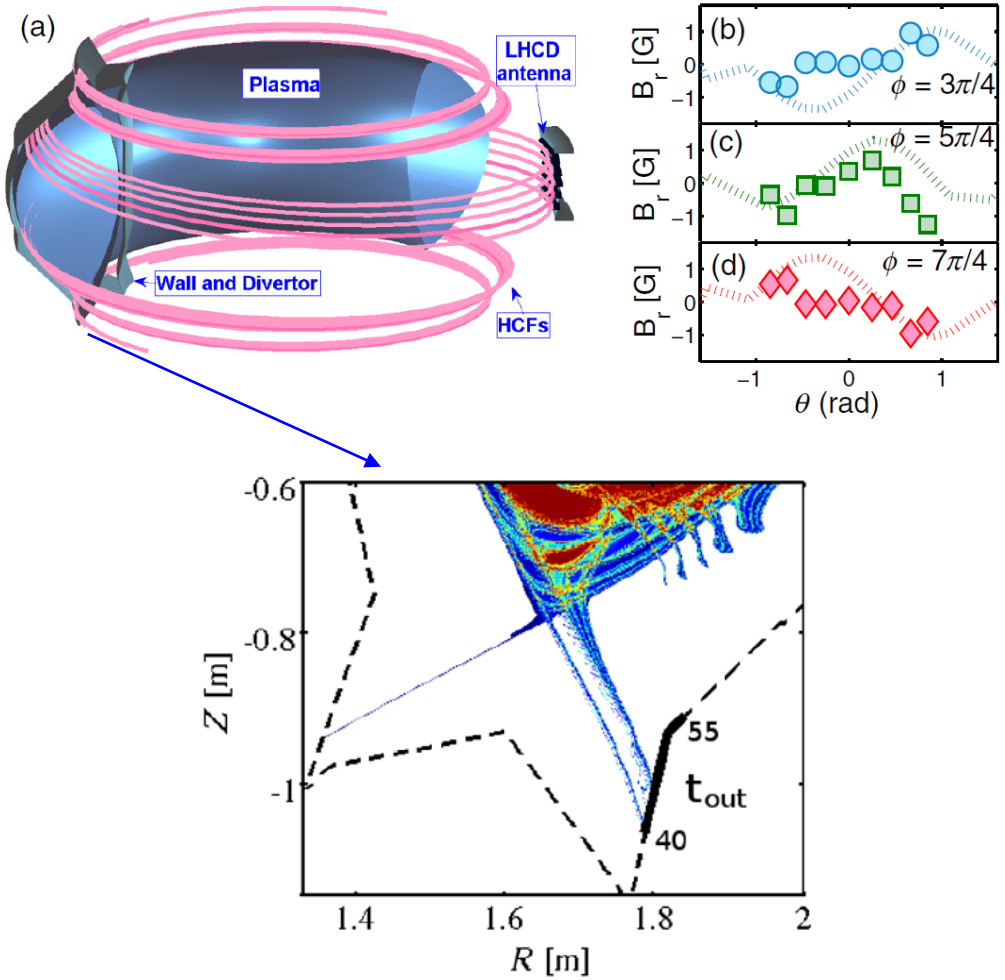

* Y.F. Liang et al., PRL 110, 235002 (2013).

ASIPP

The model of HCF in BOUT++ simulations: force free in SOL

- **Boozer, Phys. Plasmas 20, 082510 (2013): The geometry of the halo region is largely determined by :**
  The current density in the halo must have the force-free form $j_h = (j_h/B)B$, where j_h/B must be constant to make the current divergence free.

$$I_{tile} = \int \frac{j_h}{B} \vec{B} \cdot \hat{n} da,$$

- **Gerhardt, Nucl. Fusion 53 (2013) 023005:**

$$J(\phi, t) = f_0 + f_1 \cos^{2f_4}\left(\frac{\phi - f_2 - f_3 t}{2}\right).$$

- **A Guassian function type radial profile is implemented into the simulations**

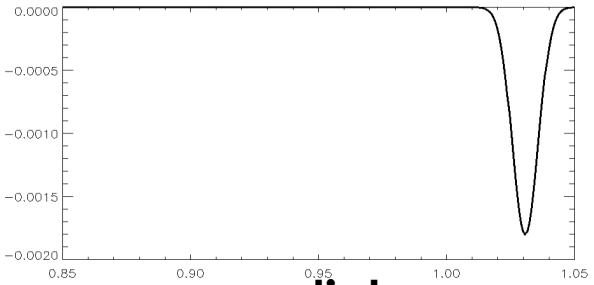

radial

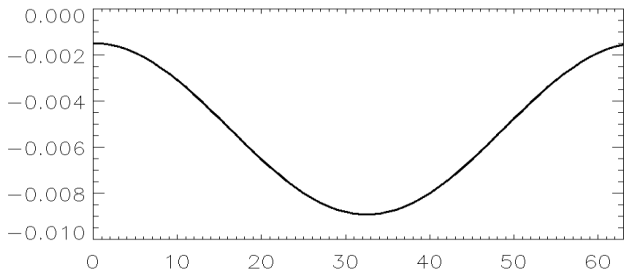

Toroidal

ASIPP

The HCF effects goes into the model as an additional magnetic flutter

$$
\begin{aligned}
\frac{\partial}{\partial t}\varpi &= -\frac{1}{B_0}\boldsymbol{b}\times\boldsymbol{\nabla}_\perp\Phi\cdot\boldsymbol{\nabla}\varpi + B_0^2\nabla_\parallel\left(\frac{J_\parallel + j_h}{B_0}\right) + 2\boldsymbol{b}\times\boldsymbol{\kappa}\cdot\boldsymbol{\nabla}p \\
&\quad -\frac{1}{2\Omega_i}\left[\frac{1}{B_0}\boldsymbol{b}\times\boldsymbol{\nabla}P_i\cdot\boldsymbol{\nabla}\left(\nabla_\perp^2\Phi\right) - Z_i e B_0\boldsymbol{b}\times\boldsymbol{\nabla}n_i\cdot\boldsymbol{\nabla}\left(\frac{\nabla_\perp\Phi}{B_0}\right)^2\right] \\
&\quad +\frac{1}{2\Omega_i}\left[\frac{1}{B_0}\boldsymbol{b}\times\boldsymbol{\nabla}\Phi\cdot\boldsymbol{\nabla}\left(\nabla_\perp^2 P_i\right) - \nabla_\perp^2\left(\frac{1}{B_0}\boldsymbol{b}\times\boldsymbol{\nabla}\Phi\cdot\boldsymbol{\nabla}P_i\right)\right] + \mu_{\parallel i}\nabla_{\parallel 0}^2\varpi, \qquad (1)\\
\frac{\partial}{\partial t}n_i &= -\frac{1}{B_0}\boldsymbol{b}\times\boldsymbol{\nabla}_\perp\Phi\cdot\nabla n_i - \frac{2n_i}{B_0}\boldsymbol{b}\times\boldsymbol{\kappa}\cdot\boldsymbol{\nabla}\Phi \\
&\quad -\frac{2}{Z_i e B_0}\boldsymbol{b}\times\boldsymbol{\kappa}\cdot\boldsymbol{\nabla}P_i - n_i B_0\nabla_\parallel\left(\frac{V_{\parallel i}}{B_0}\right), \qquad (2)\\
\frac{\partial}{\partial t}V_{\parallel i} &= -\frac{1}{B_0}\boldsymbol{b}\times\boldsymbol{\nabla}_\perp\Phi\cdot\boldsymbol{\nabla}V_{\parallel i} - \frac{1}{m_i n_{i0}}\boldsymbol{b}\cdot\boldsymbol{\nabla}P, \qquad (3)\\
\frac{\partial}{\partial t}A_\parallel &= -\nabla_\parallel\phi + \frac{\eta}{\mu_0}\nabla_\perp^2 A_\parallel + \frac{1}{e n_{e0}}\nabla_\parallel P_e + \frac{0.71 k_B}{e}\nabla_\parallel T_e - \frac{\eta_H}{\mu_0}\nabla_\perp^4 A_\parallel + \frac{\eta}{\mu_0}j_h, \qquad (4)\\
\frac{\partial}{\partial t}T_i &= -\frac{1}{B_0}\boldsymbol{b}\times\boldsymbol{\nabla}_\perp\Phi\cdot\boldsymbol{\nabla}T_i - \frac{2}{3}T_i\left[\left(\frac{2}{B_0}\boldsymbol{b}\times\boldsymbol{\kappa}\right)\cdot\left(\boldsymbol{\nabla}\Phi + \frac{1}{Z_i e n_{i0}}\boldsymbol{\nabla}P_i + \frac{5}{2}\frac{k_B}{Z_i e}\boldsymbol{\nabla}T_i\right) + B_0\nabla_\parallel\left(\frac{V_{\parallel i}}{B_0}\right)\right] \\
&\quad +\frac{2}{3n_{i0}k_B}\nabla_\parallel\left(\kappa_{\parallel i}\nabla_\parallel T_i\right) + \frac{2m_e}{m_i}\frac{Z_i}{\tau_e}\left(T_e - T_i\right), \qquad (5)\\
\frac{\partial}{\partial t}T_e &= -\frac{1}{B_0}\boldsymbol{b}\times\boldsymbol{\nabla}_\perp\Phi\cdot\boldsymbol{\nabla}T_e - \frac{2}{3}T_e\left[\left(\frac{2}{B_0}\boldsymbol{b}\times\boldsymbol{\kappa}\right)\cdot\left(\boldsymbol{\nabla}\Phi - \frac{1}{e n_{e0}}\boldsymbol{\nabla}P_e - \frac{5}{2}\frac{k_B}{e}\boldsymbol{\nabla}T_e\right) + B_0\nabla_\parallel\left(\frac{V_{\parallel e}}{B_0}\right)\right] \\
&\quad +0.71\frac{2T_e}{3e n_{e0}}B_0\nabla_\parallel\left(\frac{J_\parallel + j_h}{B_0}\right) + \frac{2}{3n_{e0}k_B}\nabla_\parallel\left(\kappa_{\parallel e}\nabla_\parallel T_e\right) - \frac{2m_e}{m_i}\frac{1}{\tau_e}\left(T_e - T_i\right) \\
&\quad +\frac{2}{3n_{e0}k_B}\eta_\parallel\left(J_\parallel + j_h\right). \qquad (6)
\end{aligned}
$$

$$
\nabla_\parallel = \nabla_{\parallel 0} - \boldsymbol{b}_0\times\boldsymbol{\nabla}A_\parallel/B_0 - \boldsymbol{b}_0\times\boldsymbol{\nabla}A_h/B_0
$$

ASIPP

The simulations reproduce the splitting of the strike point by helical filamentary current (HCF)

- HCFs dominated by n=1, but n>1 used in the simulation due to the efficiency
- SOL width λ_q is indeed broadened by HCFs
- The splitting of strike point behavior is reproduced

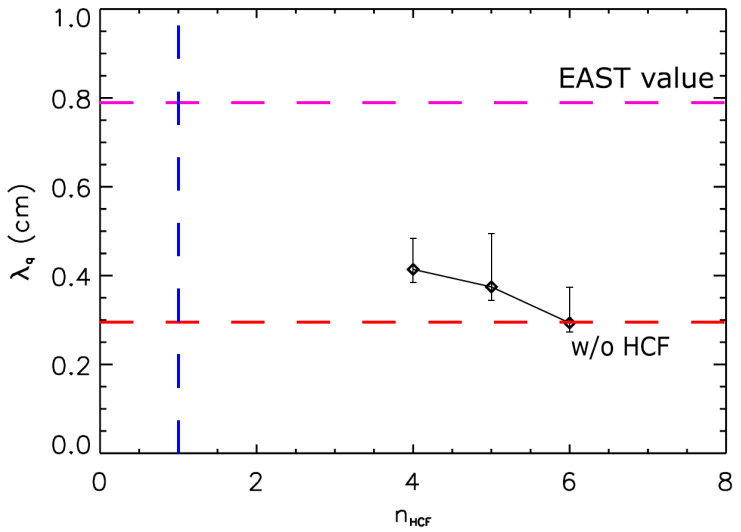

HCF broadens SOL width

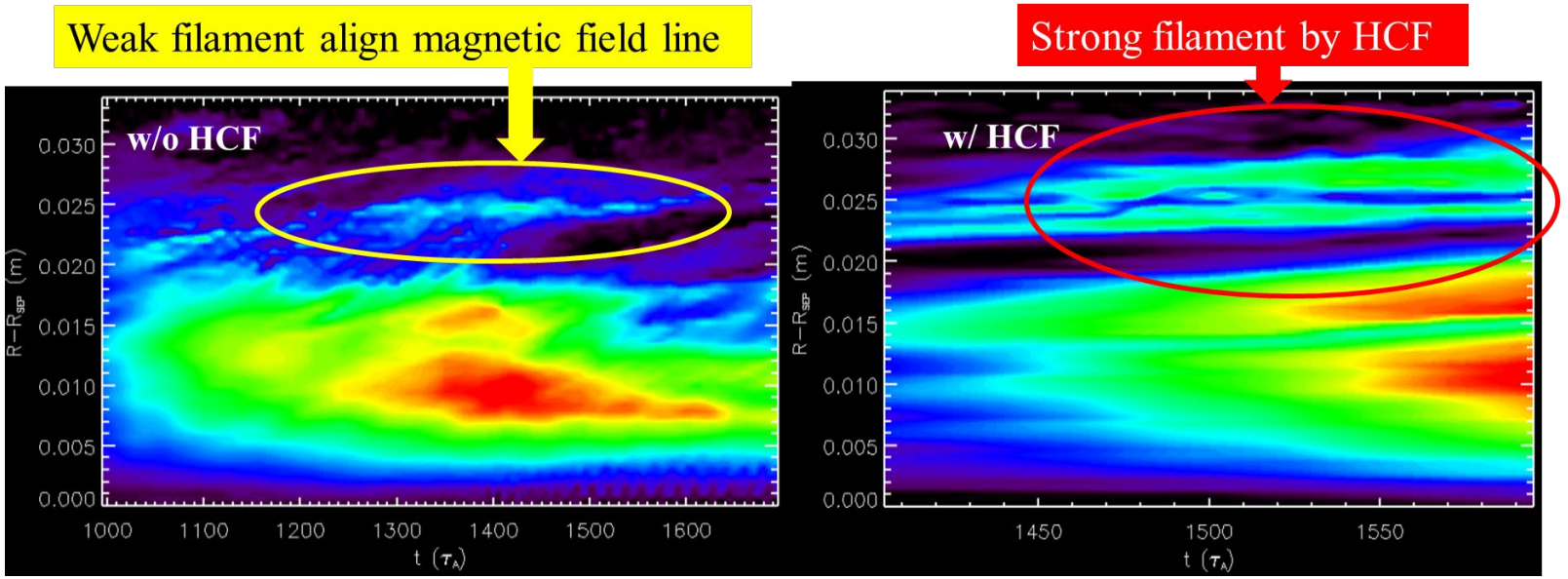

T.Y. Xia et al., NF 59 076043 (2019)

ASIPP

Turbulence enhancement is found to be effective for ELM mitigation

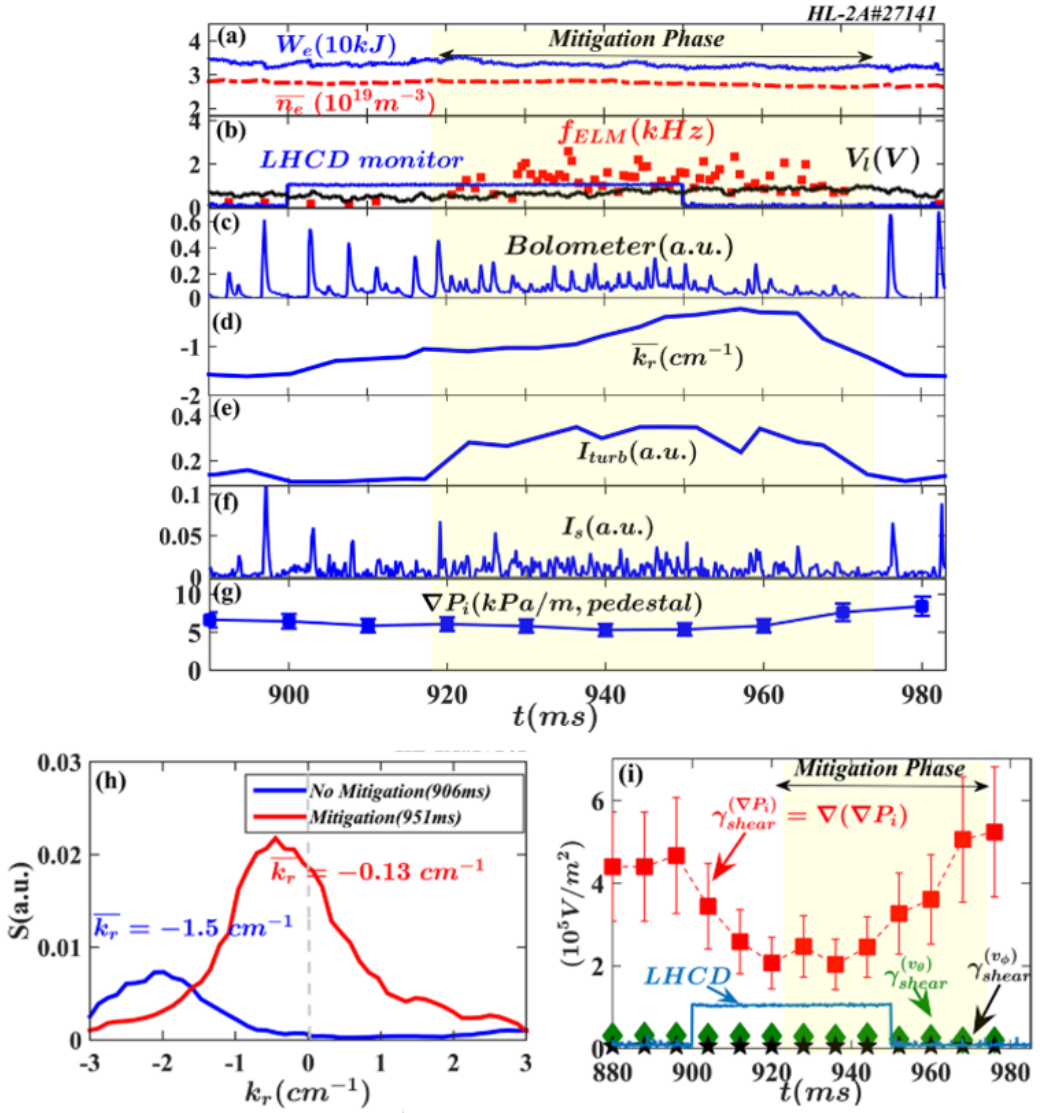

LHW modified the pedestal ion pressure gradient

↓

A reduction of the ion diamagnetic term of the edge E×B velocity shear

↓

The kr of the pedestal turbulence shifted

↓

The pedestal turbulence is enhanced

↓

ELM mitigation

G.L. Xiao, et al., Nucl. Fusion 59 (2019) 126033

ASIPP

An EAST ELMy H-mode discharge is used for the simulations

Simulation domains & profiles: EAST#77741@5.1s

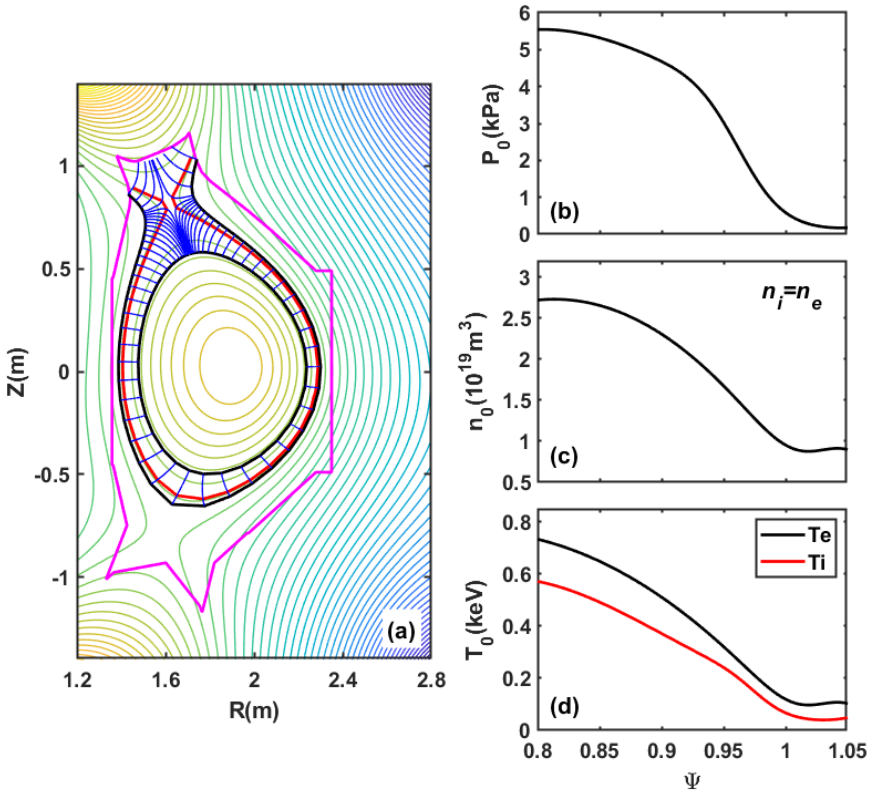

- Equilibrium is reconstructed by k-EFIT
- Simulation domain includes pedestal & SOL

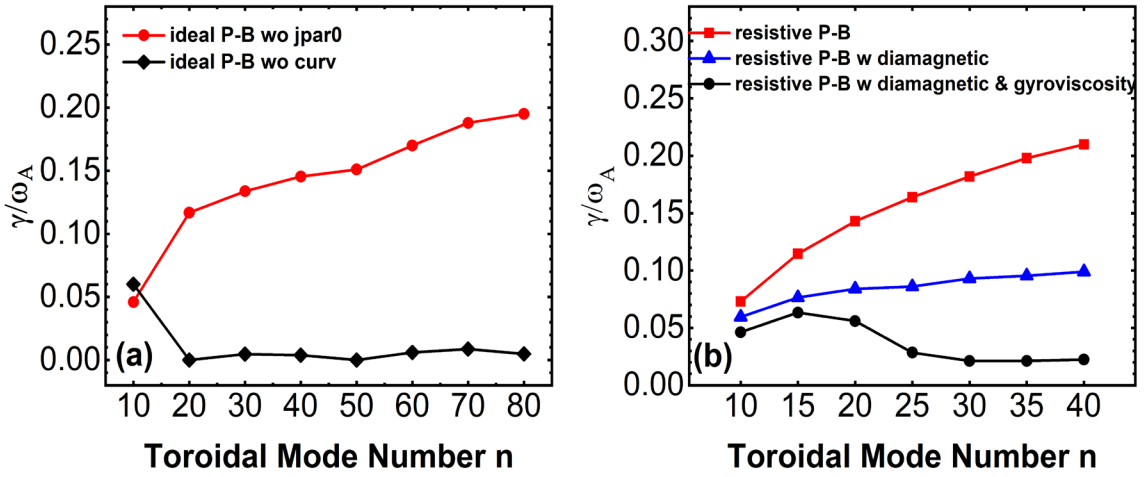

- The equilibrium is ideal ballooning unstable
- RBM is unstable, but not important
- FLR stabilizes the high n mode

ASIPP

The direct simulations obtains a large ELM & QCM

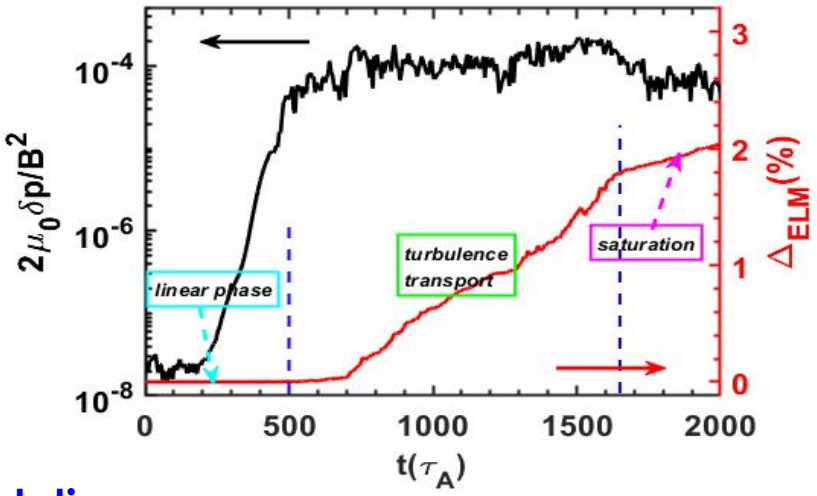

Simulations:

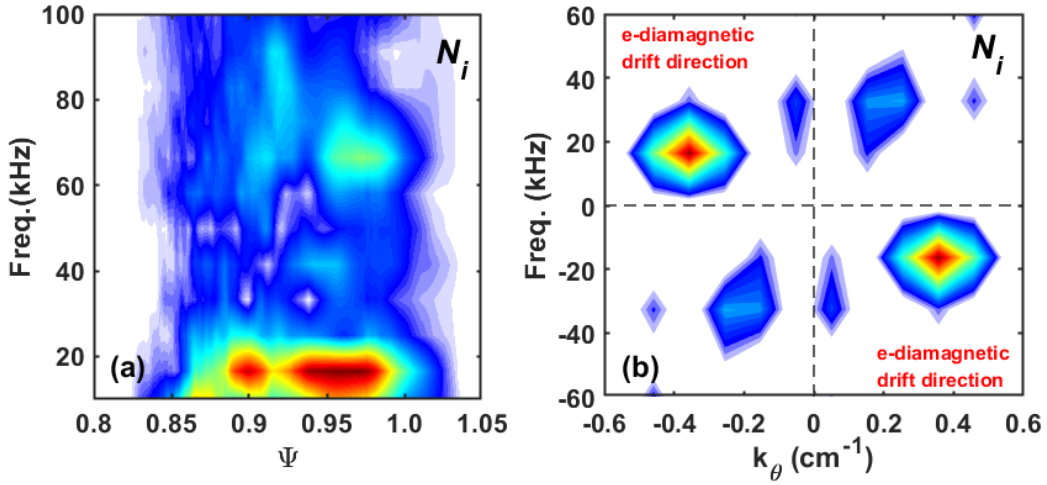

Nonlinear simulations:

- ELM size >2%, large ELM
- Saturated fluctuation amplitude: ~10^{-4}
- A QCM is found after ELM crash, on e-diamagnetic direction
- f_{QCM}~20kHz, similar to the Li-BES diagnostic

Diagnostic:

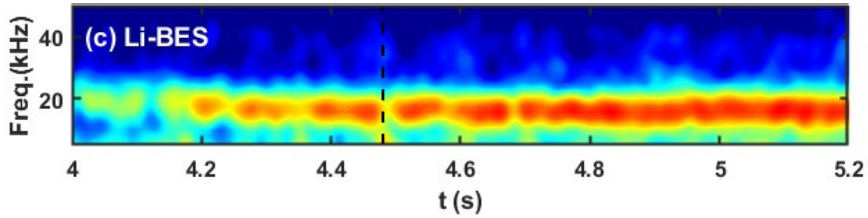

Focusing on the interaction between turbulence and ELM

A modelled PCM is able to decrease ELM size

A modelled pedestal coherent mode is added into BOUT++:

$$\tilde{P}_{CM}(\mathrm{x,y,z,A}) = \mathbf{A}\cdot e^{-\frac{(x-b_1)^2}{2\sigma_x^2}-\frac{(y-b_2)^2}{2\sigma_y^2}}\left[\overline{P}_{kz}(n)e^{-i\theta}\right]_{IFT}.$$

$$\frac{\partial \varpi}{\partial t} + V_E\cdot\nabla\varpi = B_0\nabla_{\parallel}J_{\parallel} + 2\overrightarrow{b_0}\times\overrightarrow{\kappa_0}\cdot\nabla\left(P+\tilde{P}_{CM}\right)$$

$$\frac{\partial P}{\partial t} + V_E\cdot\nabla P = -V_E\cdot\nabla\tilde{P}_{CM}$$

$$\varpi = \frac{n_0 M_i}{B_0}\left[\nabla_{\perp}^2\phi + \frac{1}{n_0 Z_i e}\nabla_{\perp}^2\left(P+\tilde{P}_{CM}\right) + \frac{\nabla n_0}{n_0}\cdot\nabla\phi\right]$$

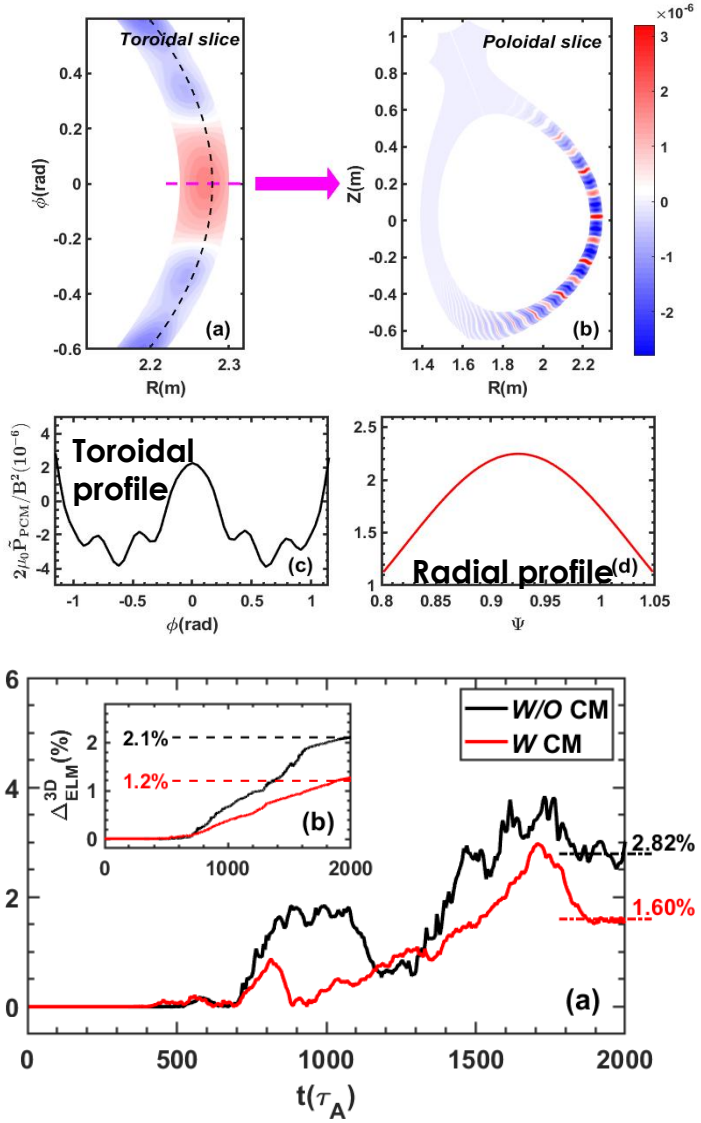

- For better scan of the key parameters,
- ELM size is decreased by ~43%

ASIPP

Mechanism: nonlinear interactions limit the saturation amplitude of ELM

- **Similar mechanism for HCF and CM:**
  Nonlinear mode interactions among multi modes driven by HCF Br or CM decrease the phase coherent time (P.W. Xi, PRL, 2014) and leads to the slow growing.
- **Difference:**
  initial magnetic perturbation for HCF;
  initial electrostatic perturbation for PCM

HCF:

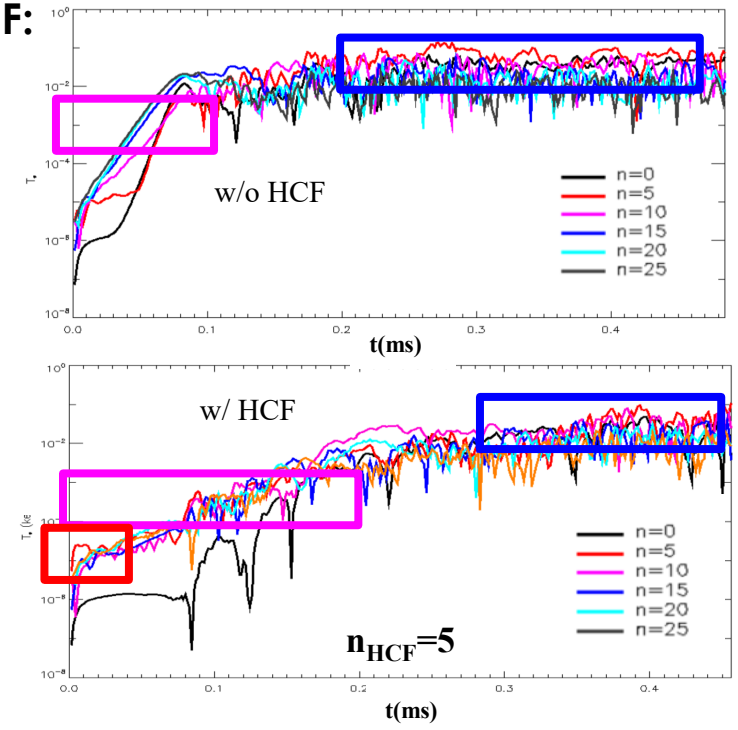

PCM:

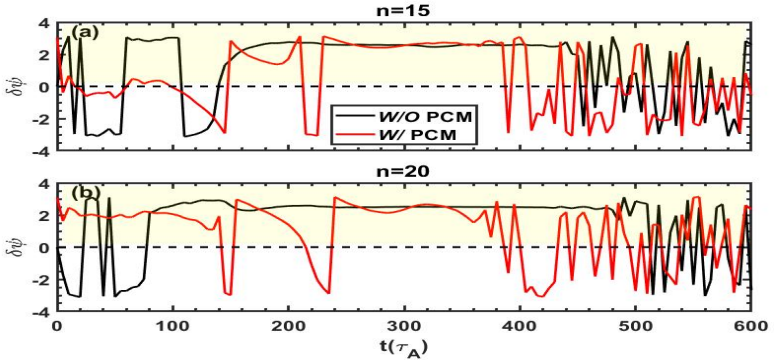

phase coherent time is shortened by PCM

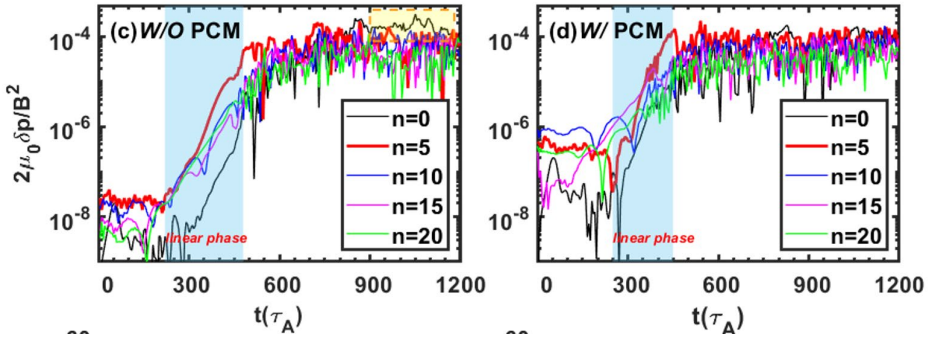

ASIPP

The key parameter scan show a threshold of PCM amplitude for ELM mitigation

Amplitude scan

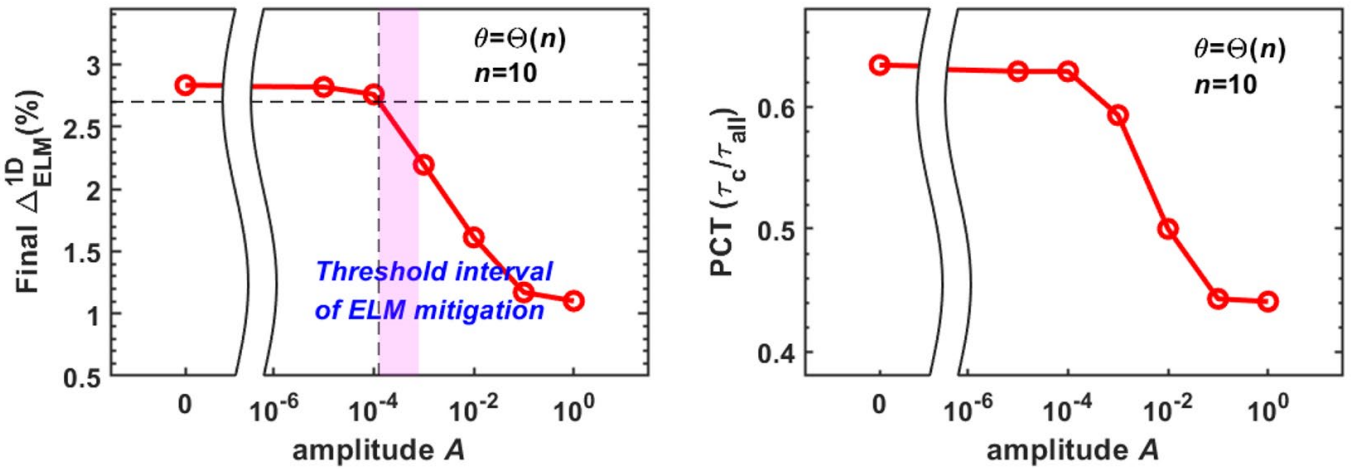

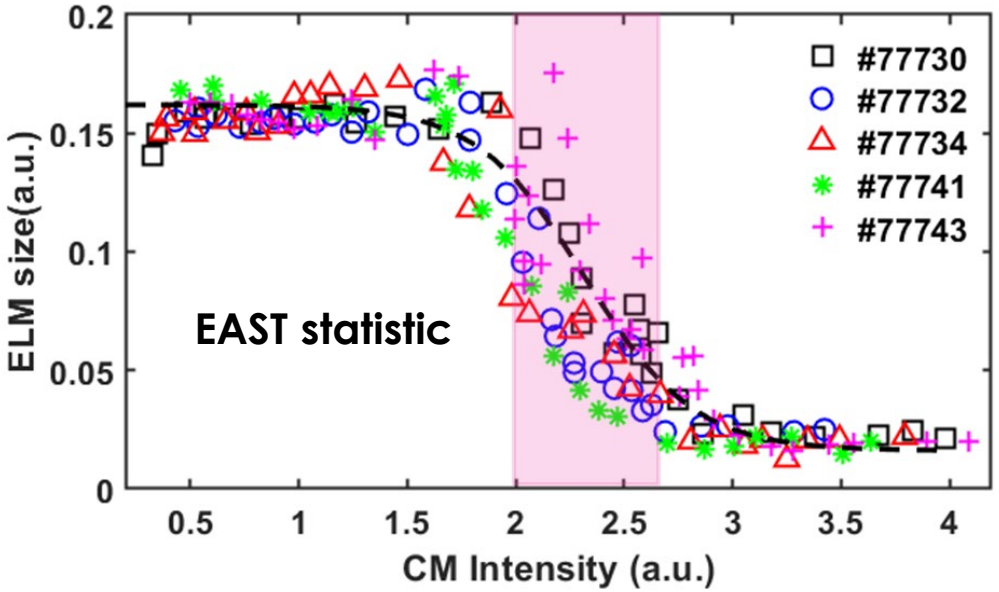

- The ELM size trends to be smaller when the A becomes larger than the threshold
- The trend of PCT is same to ELM size
- Consistent with the EAST experiments

Y.L. Li et al., NF 62 066043 (2022)

ASIPP

ICW is found to suppress ELM on EAST for the first time

EAST finds that ICWs are able to suppress ELMs without too much change of pedestals.

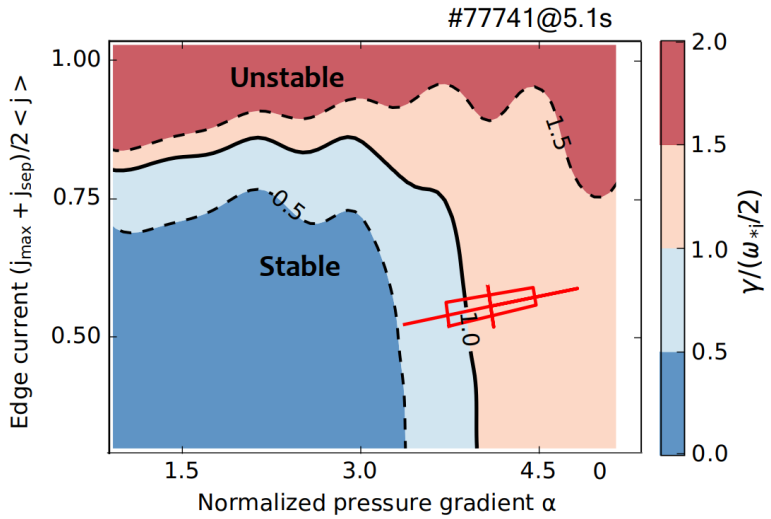

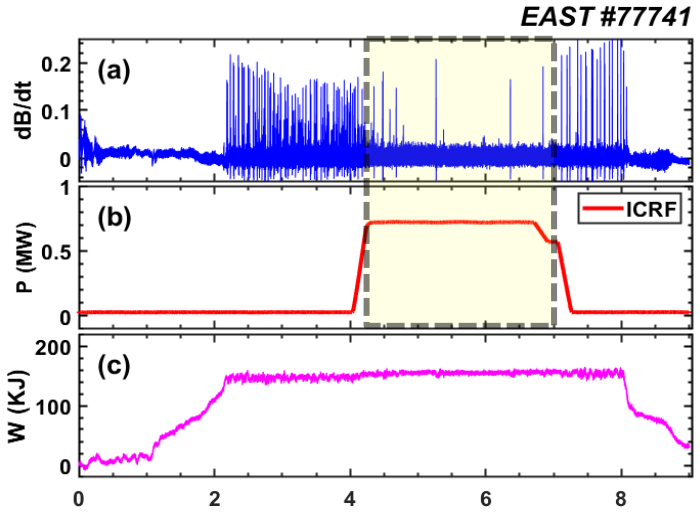

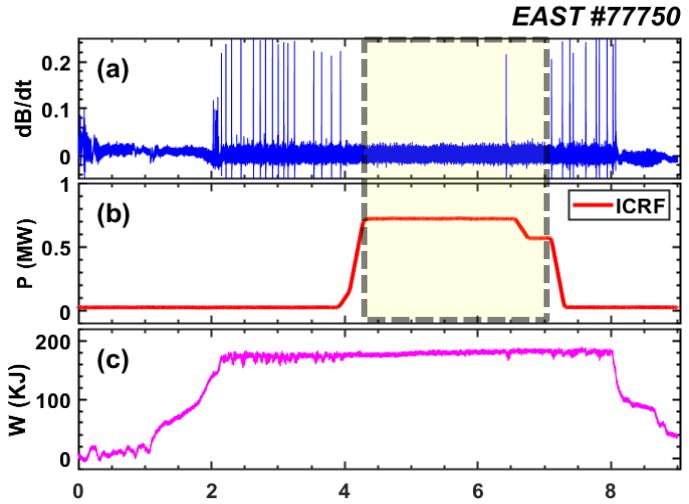

Both linear and nonlinear simulations show that the pedestal leads to ELMs, no mitigation.

X.J. Zhang et al., Sci. China-Phys. Mech. Astron. 65(3): 235211 (2022)

ASIPP

RF sheath potential module is developed to calculate the SOL radial electric field in tokamaks

The RF sheath located near the antenna region for RF heating scheme
A minimal 2-field model is developed in BOUT++ framework

RF sheath:

$$\phi_B = \frac{T_e}{e}\ln\left(\frac{v_{Te}}{2\sqrt{\pi}C_s}\right) = \frac{T_e}{e}\frac{1}{2}\ln\left(\frac{m_i}{m_e}\frac{2T_e}{T_i+T_e}\frac{1}{4\pi}\right)$$

2-field model:

$$\begin{cases} \dfrac{\partial \varpi}{\partial t} = B_0\nabla_\parallel J_\parallel + \mu_{i,\perp}\nabla_\perp^2\varpi + \mu_{i,\parallel}\nabla_\parallel^2\varpi \\ \varpi = \dfrac{n_0 M_i}{B_0}\left(\nabla_\perp^2\phi + \dfrac{1}{n_0 Z_i e}\nabla_\perp^2 P_i\right) \\ J_\parallel = -\dfrac{1}{\eta}\nabla_\parallel\phi + \dfrac{1}{\eta e n_e}\nabla_\parallel P_e + \dfrac{0.71k_B}{\eta e}\nabla_\parallel T_e \end{cases}$$

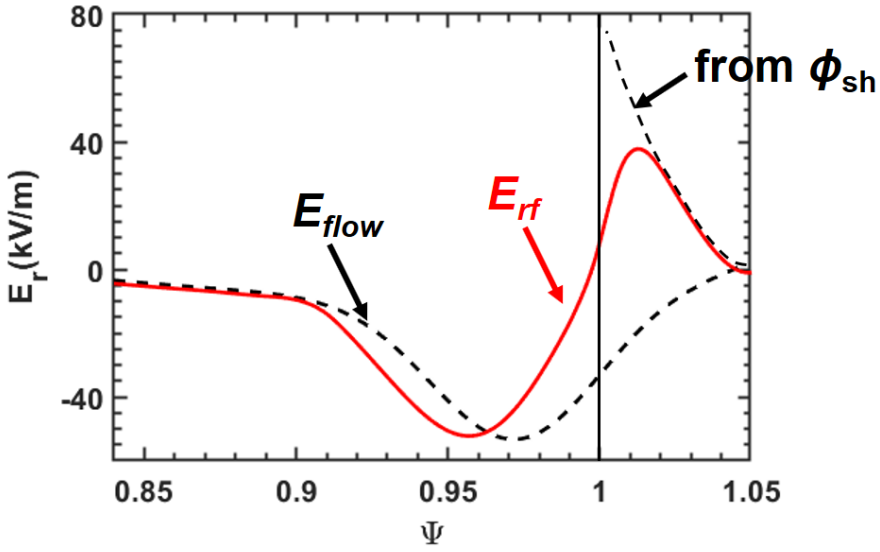

- A positive Er forms in SOL.
- Smoothly connected across the separatrix to the force-balanced Er in pedestal.

Gui, B., et al. Nuclear Fusion 58 026027 (2018).

ASIPP

Shear effects by RF sheath leads to the suppression of ELMs

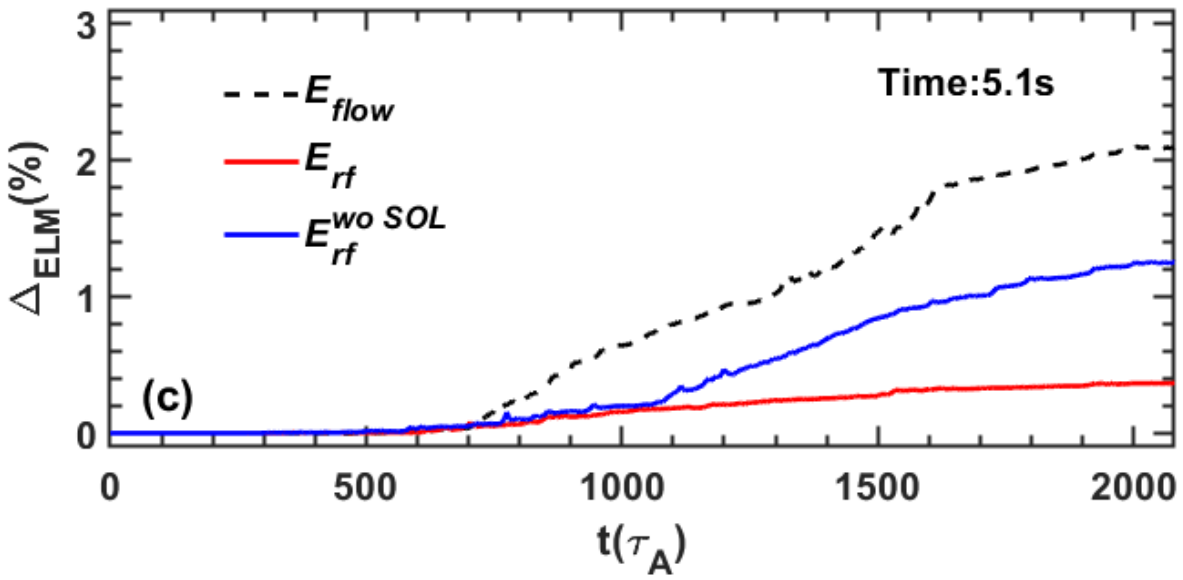

算例	E_{flow}	$E_{rf}^{wo\_sol}$	E_{rf}
$\Delta_{\mathrm{ELM}}^{3\mathrm{D}}$	2.1%	1.23%	0.36%

- The ELM size is effectively decreased by RF sheath
- The shear effects in SOL is important

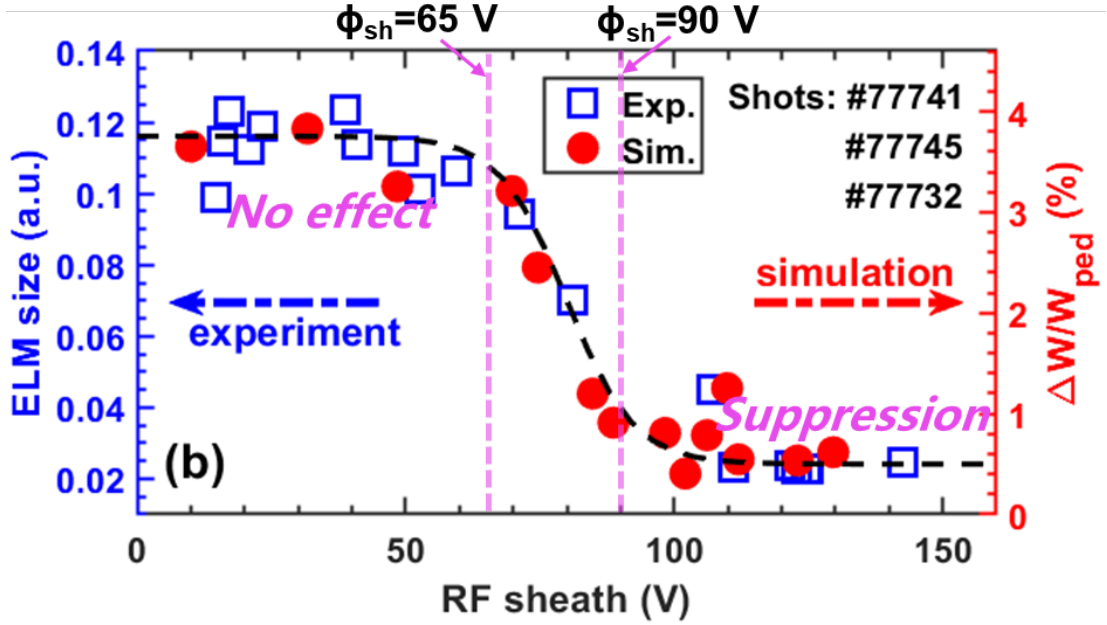

- The suppression window is found in simulations
- Consistent with experiments

Also See in Jan. 12:
The simulation of ELMs suppression by ion cyclotron resonance heating in EAST using BOUT++

Y.L. Li, et al. Nuclear Fusion 62 066018 (2022).

ASIPP

Outline

- Motivation
- Modeling for RF effects on ELM control
- **Modeling for magnetic topology on ELM control**
  - **RMP & QSF**
- summary

ASIPP

The plasma response module is developed in BOUT++ framework

- EAST has used multiple-n RMP coils to achieve the mitigation of ELMs
- A simplest 2-field reduced model with relaxation method are developed to describe the plasma response to RMP
- Advantage: including toroidal coupling, easily coupled to varies of 2-fluid modules in BOUT++
- Disadvantage: unstable to kink mode
- In order to benchmark with MAPS & MARS-F, an interface between BOUT++ & MAPS are developed:
  1. Map field-aligned to PEST coordinate
  2. Interpolation data from BOUT++ to MAPS

$$\frac{\partial \tilde{\varpi}}{\partial t} = B_0 \nabla_\parallel J_\parallel + \mu_{i,\parallel} \partial^2_{\parallel 0} \tilde{\varpi}$$

$$\frac{\partial \tilde{A}_\parallel}{\partial t} = -\nabla_\parallel \tilde{\phi} + \frac{\eta}{\mu_0} \nabla^2_\perp \tilde{A}_\parallel$$

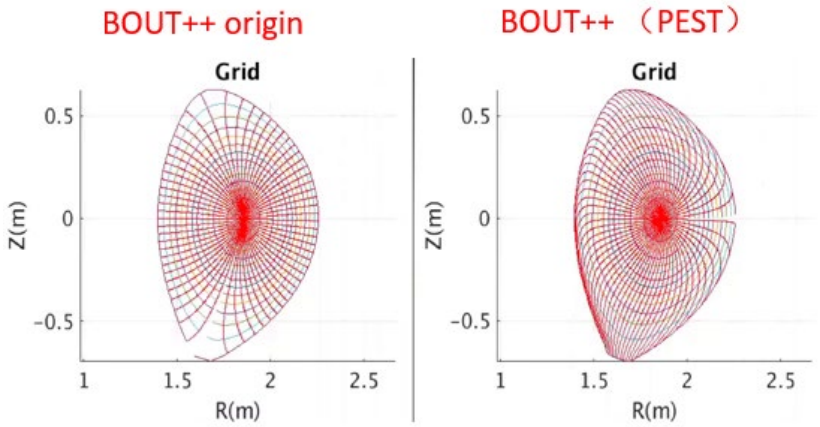

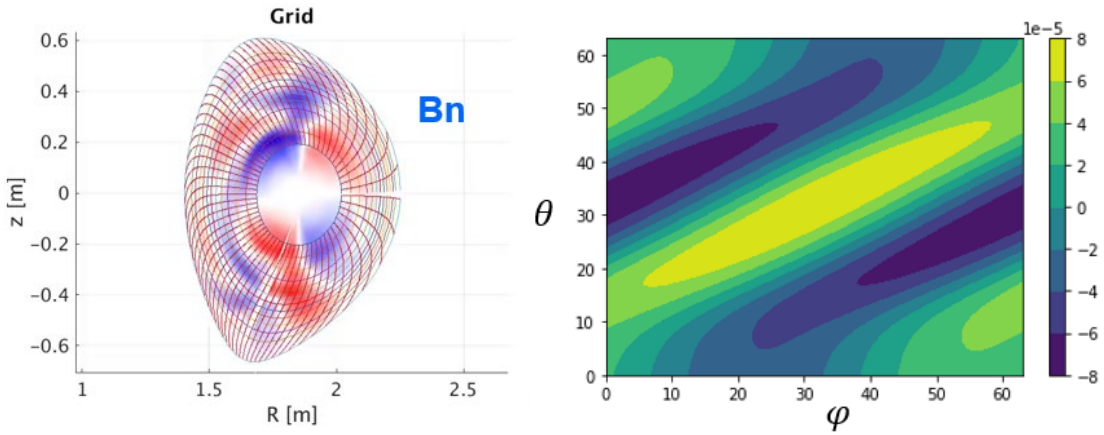

Interpolate Bn from BOUT++ to MAPS

Testing of the model: the vacuum field calculation

- **High resolution is necessary for the vacuum spectrum**

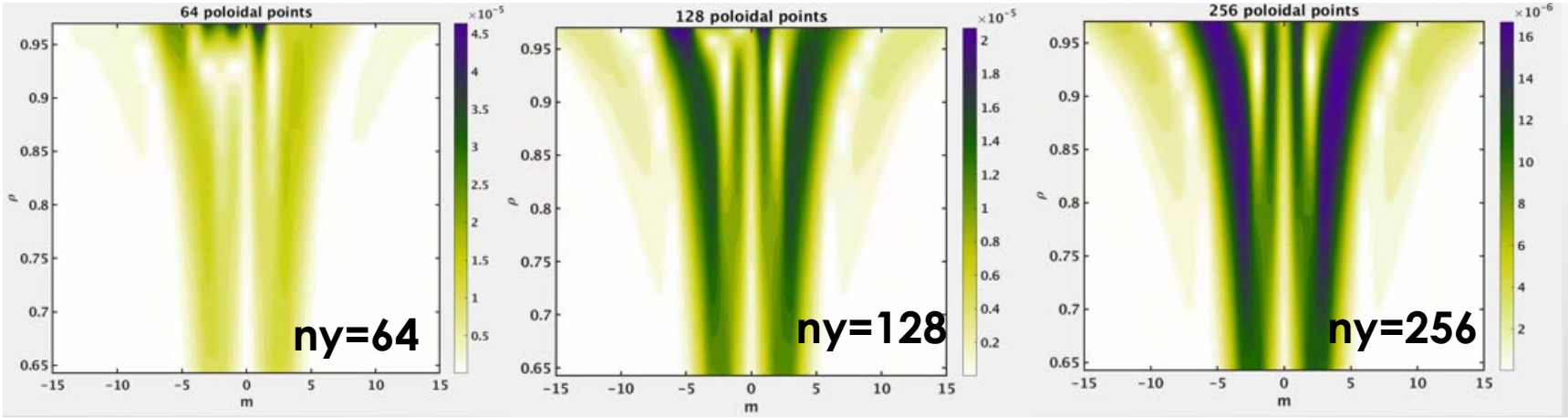

- **Spectrum for vacuum field is consistent with MAPS**

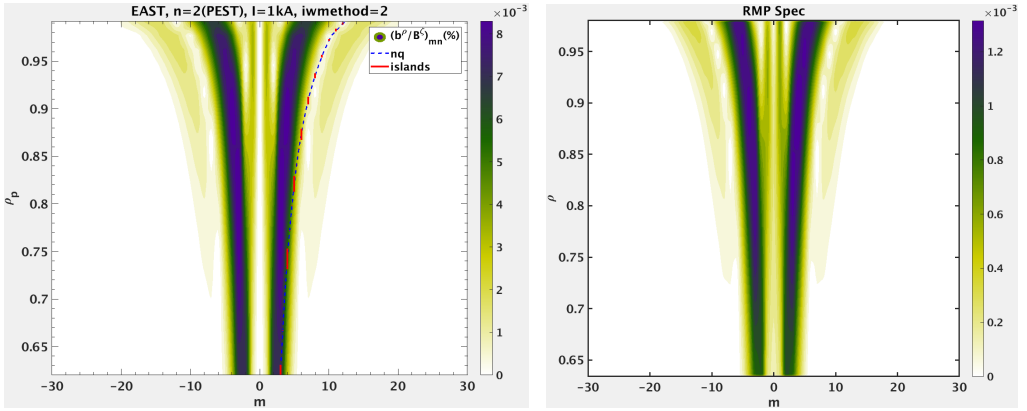

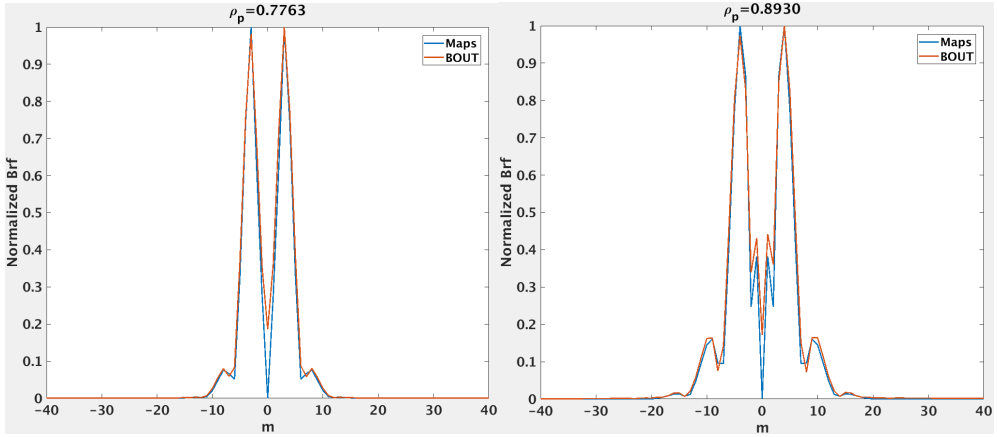

ASIPP

Response spectrum by RMP are calculated reasonably

- Using the shifted circular geometry to test the plasma response
- Screening in low resistivity and penetration in high resistivity are reproduced

- Preliminary simulations on RMP effects with ELM show: vacuum field behaves differently with response field

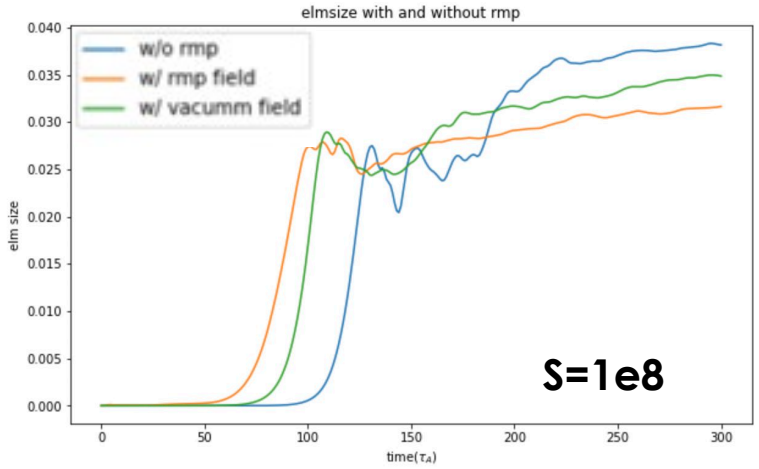

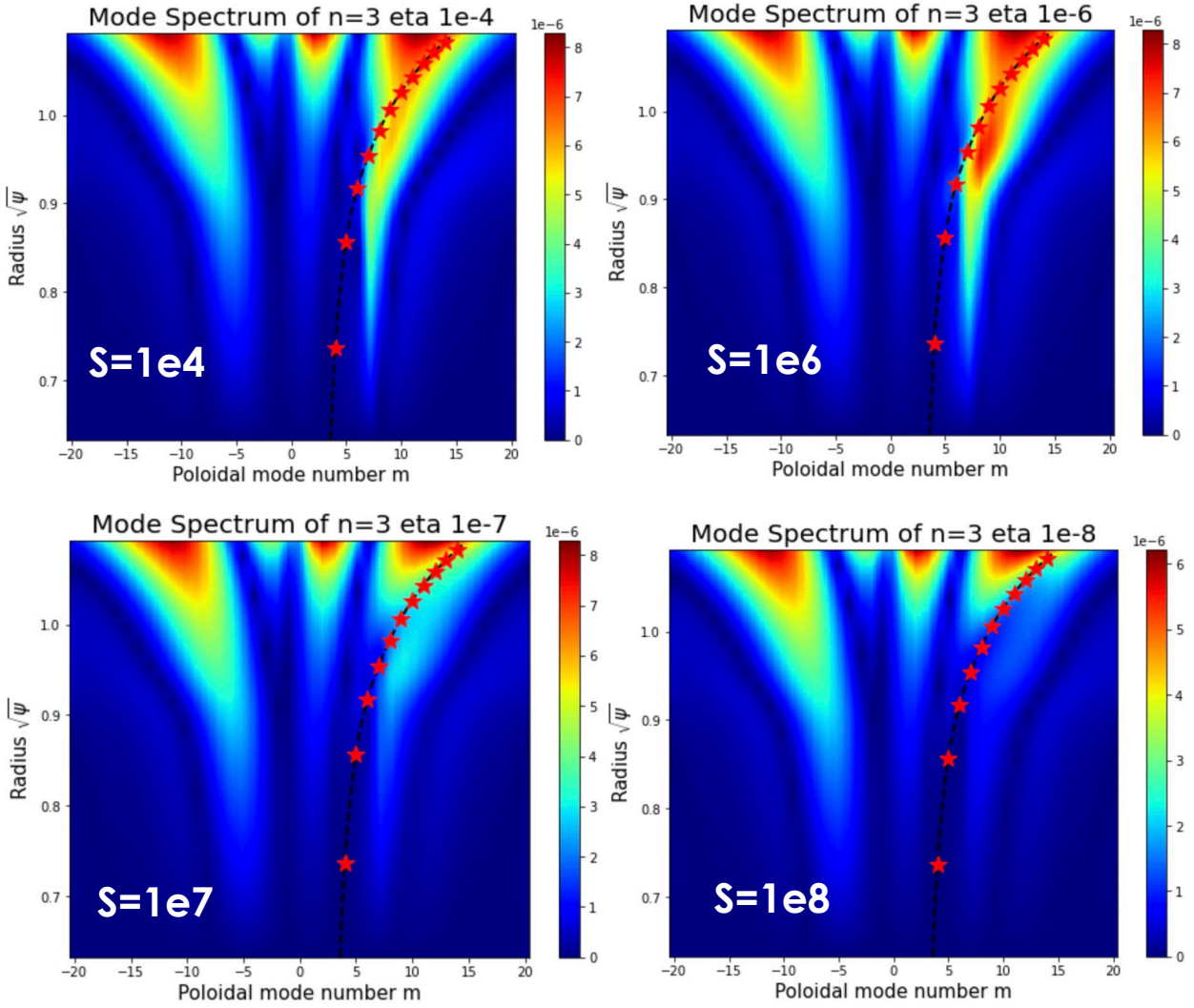

ASIPP

Snow-flake divertor may leads to the suppression or enhanced ELMs

- **EAST: ELMs are suppressed with QSF configuration.**

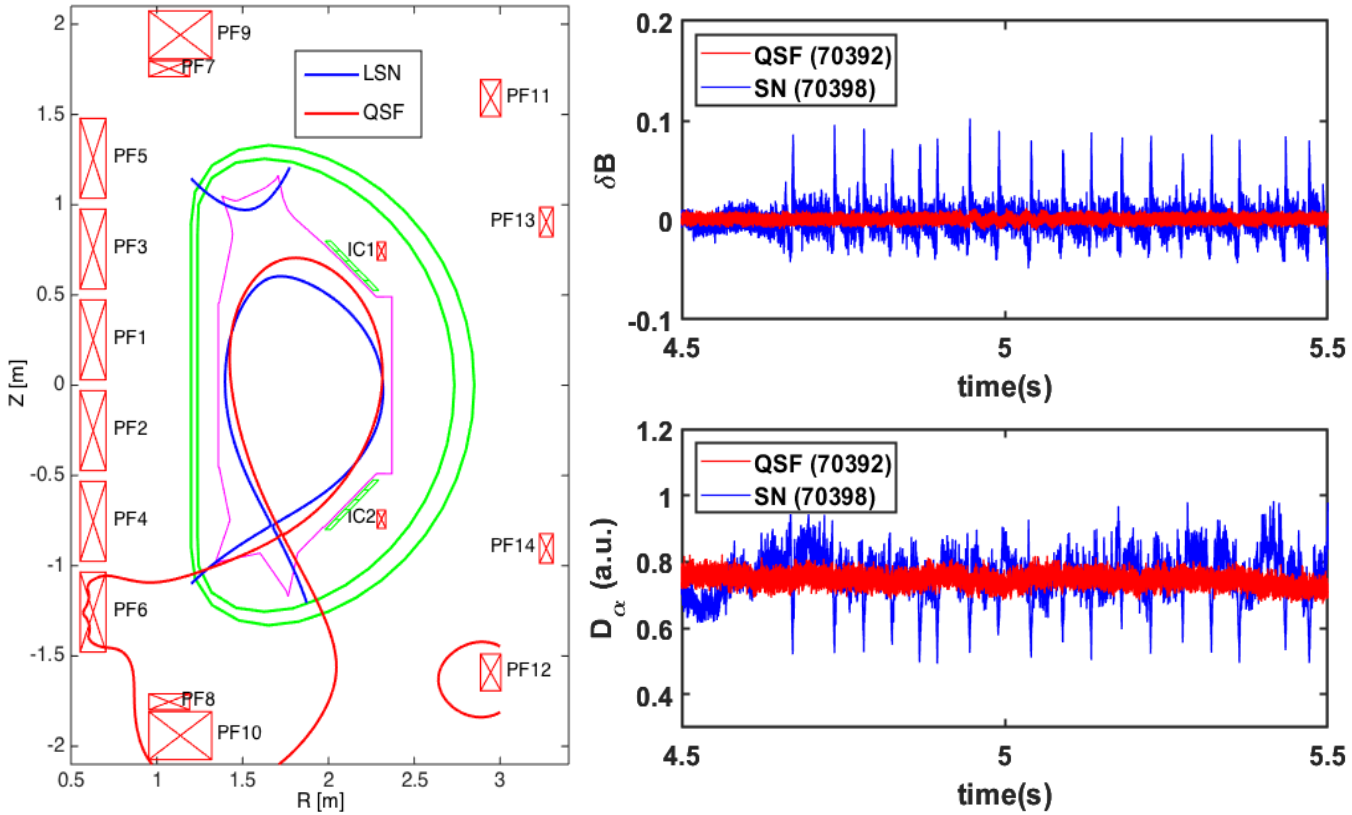

- **TCV: SF-plus can trigger larger ELMs.**

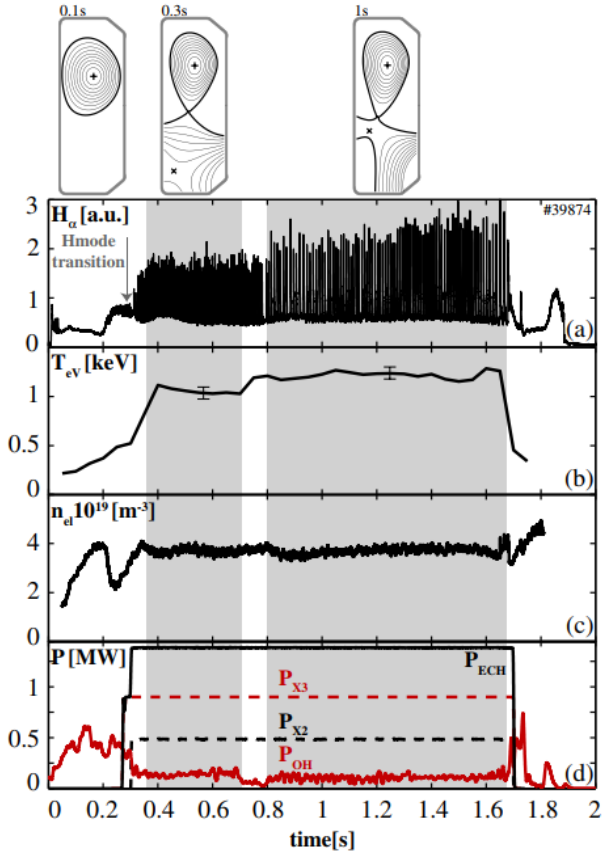

[Piras, F. et al. PRL (2010)].

ASIPP

Using K-EFIT to generate series of EAST QSF geometries

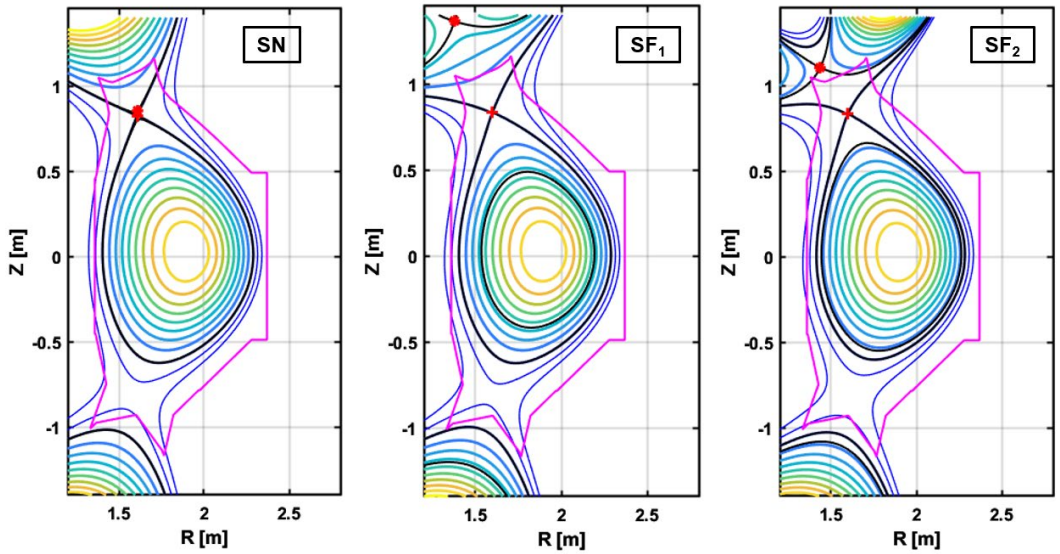

- Based On one SN EAST H-mode discharge
- Modified K-EFIT with additional fake PF coil to generate 2nd X-point
- The linear growth rate is closely related to the position of 2nd X-point.
- Essentially, the different 2nd X-point changes the local magnetic shear, thereby affecting the growth rate of P-B mode

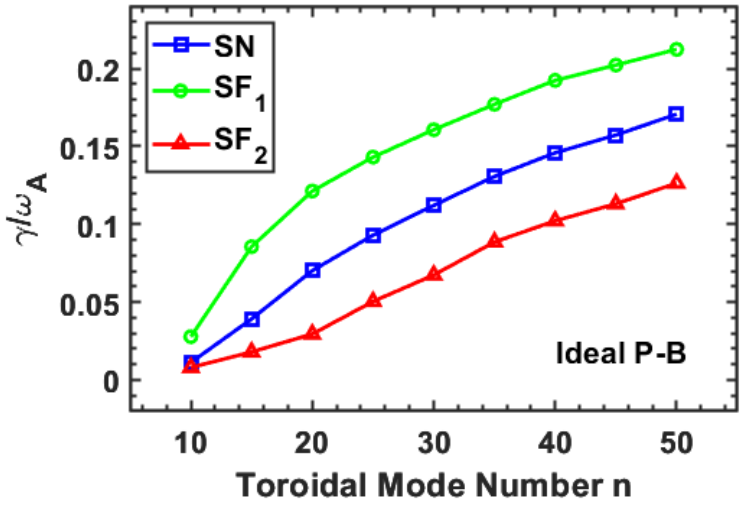

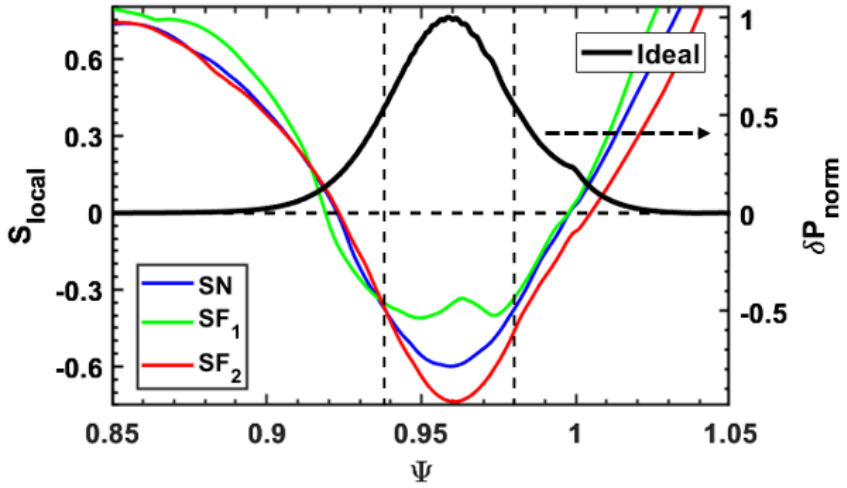

- Local magnetic shear:

$$s = \frac{r}{\nu}\frac{\partial \nu}{\partial r} \quad , \nu = \frac{rB_t}{RB_p}$$

Position scan of the 2nd X-point on EAST: local magnetic shear affects the mitigation of ELMs

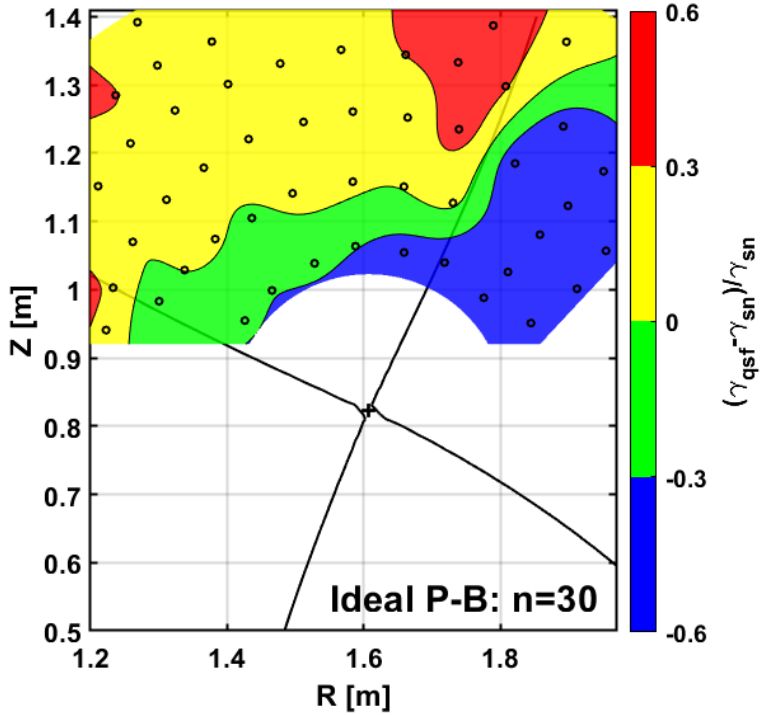

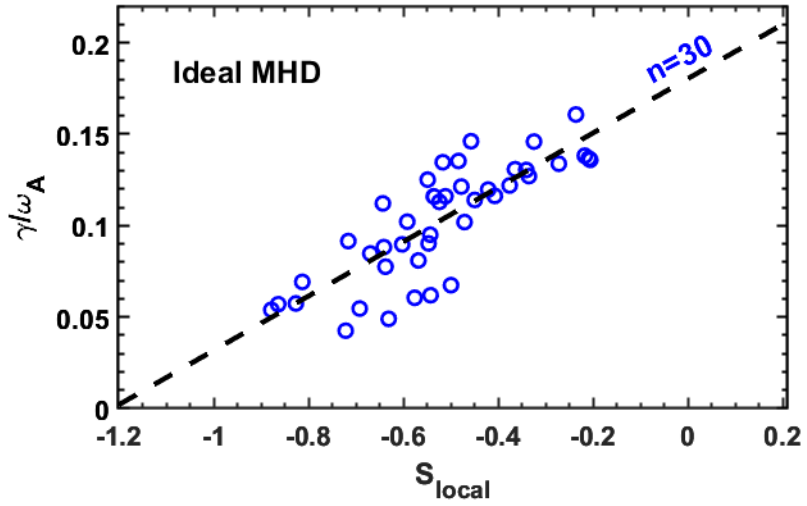

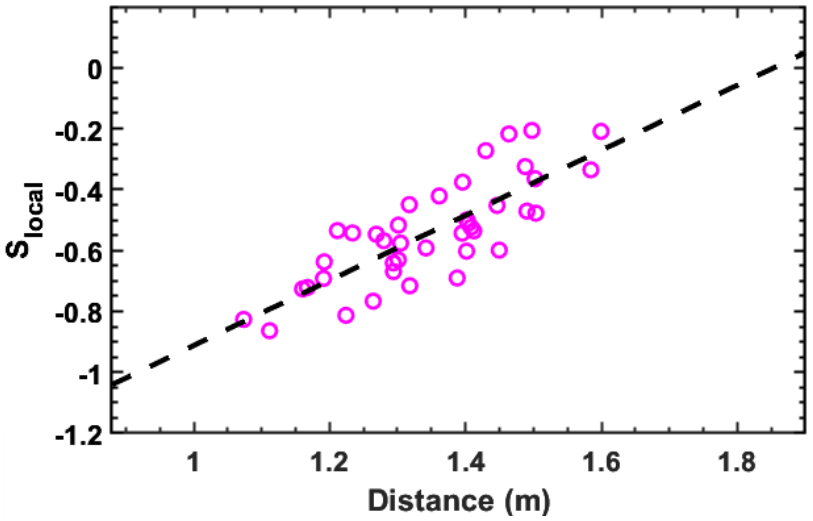

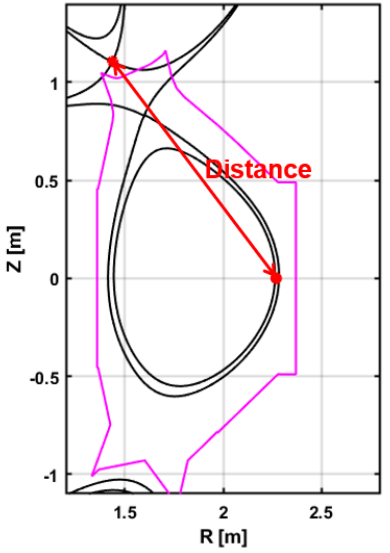

- The absolute value of local magnetic shear is inversely related to the growth rate of P-B mode.
- The distance between the second X-point and the peak pressure gradient at outer mid-plane is decreased, and the growth rate is decreased.

ASIPP

Summary

- EAST team focus on the code development and application on the physics understanding of ELM active control used on EAST

- Some of the direct RF effects are implemented in BOUT++:
  - ✓Magnetic (HCF) & electrostatic (CM) fluctuations lead to the mitigation of ELM by nonlinear interactions
  - ✓RF sheath leads to the large flow shear which can suppress ELMs

- The magnetic topology effects are underdeveloped:
  - ✓Response module for RMP field is underdeveloped
  - ✓ Scan of 2nd X-point of QSF on EAST

ASIPP


Thank you!
THOMSON DIAGNOSTIC
EAST偏振干涉仪诊断

The coherent modes at pedestal are able to mitigate ELM

- A modeled pedestal coherent mode (PCM) is added in BOUT++ to simulate the interactions with ELM.

$$\tilde{P}_{PCM}(x,y,z,A) = Af(z)\cdot e^{-\frac{(x-b_1)^2}{2\sigma_x^2}-\frac{(y-b_2)^2}{2\sigma_y^2}}.$$

$$f(z) = [F(n,\theta)]_{IFFT}.$$

$$\tilde{P}_{PCM}(x,y,z,A) = A\cdot e^{-\frac{(x-b_1)^2}{2\sigma_x^2}-\frac{(y-b_2)^2}{2\sigma_y^2}}\left[P_{kz}(n)e^{-i\theta}\right]_{IFFT}.$$

- A threshold of the amplitude of PCM is found for ELM mitigation
- Phase angle and dominant toroidal mode can also affect ELM.

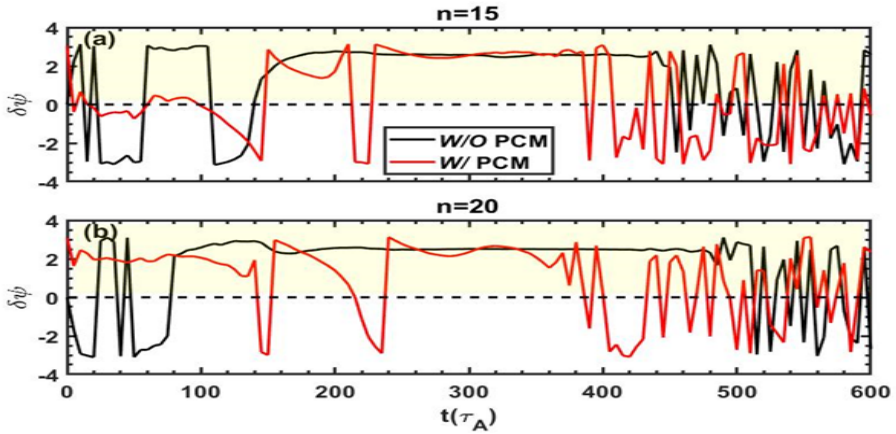

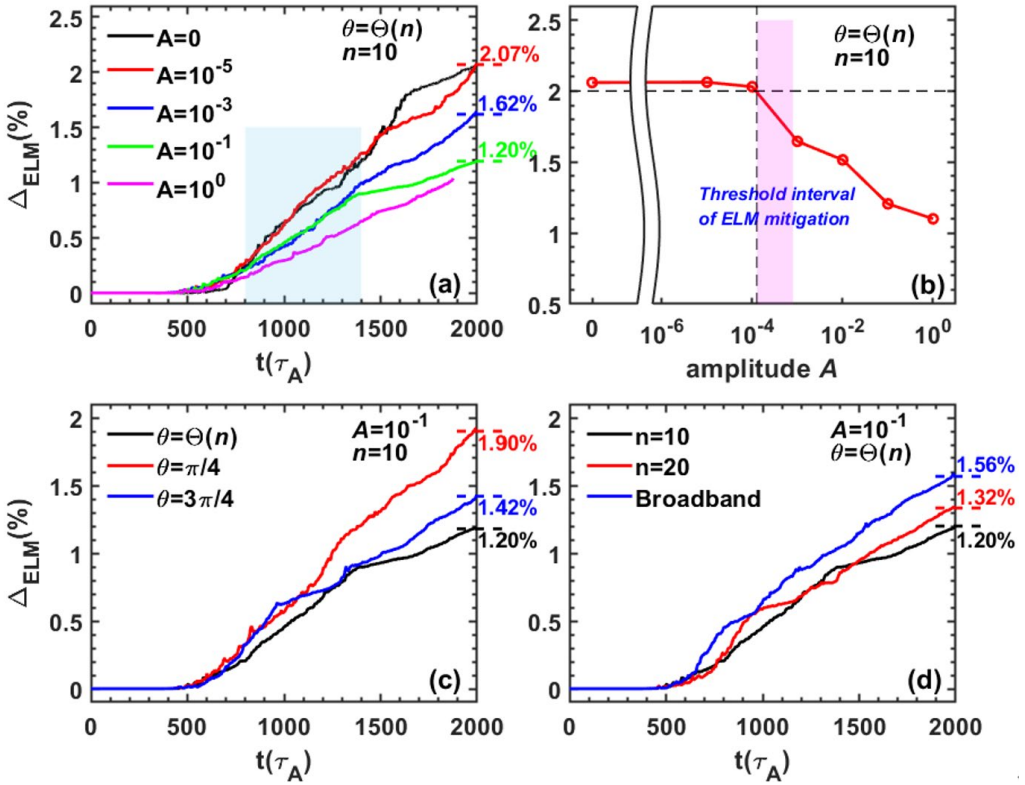

- The phase coherent time* is changed by the nonlinear wave-wave interactions in the linear phase, which change the growth time of the ELM.

Y.L. Li et al., submitted to NF

*P.W. Xi, X.Q. Xu and P.H. Diamond, 2014 PRL 112

➢ ELM size:

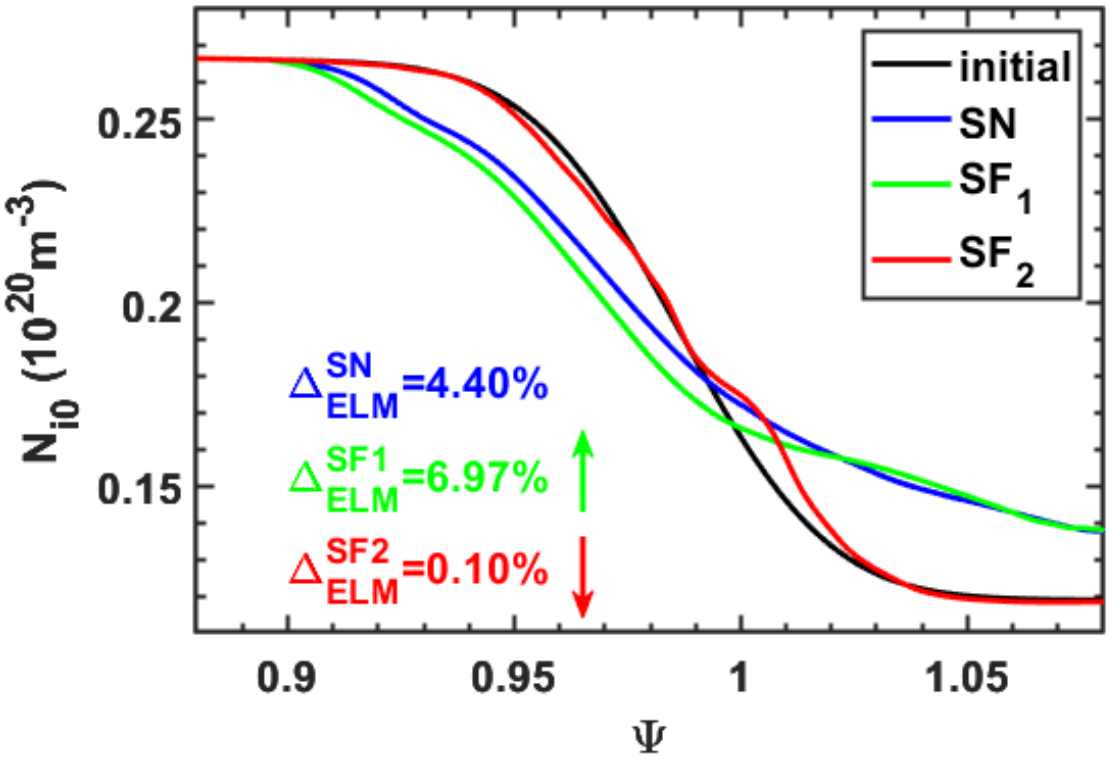

The evolution of ion density profile for different magnetic configuration

- **The ELM sizes are calculated using the pressure profiles.**
- **The strong local magnetic shear can effectively reduce the ELM energy loss.**

ASIPP